

Review

Open Access



Solidification for solid-state lithium batteries with high energy density and long cycle life

Zhijie Bi, Xiangxin Guo*

College of Physics, Qingdao University, Qingdao 266071, Shandong, China.

Correspondence to: Prof. Xiangxin Guo, College of Physics, Qingdao University, No. 308 Ningxia Road, Shinan District, Qingdao 266071, Shandong, China. E-mail: xxguo@qdu.edu.cn

How to cite this article: Bi Z, Guo X. Solidification for solid-state lithium batteries with high energy density and long cycle life. *Energy Mater* 2022;2:200011. <https://dx.doi.org/10.20517/energymater.2022.07>

Received: 5 Mar 2022 **First Decision:** 8 Apr 2022 **Revised:** 15 Apr 2022 **Accepted:** 18 Apr 2022 **Published:** 24 Apr 2022

Academic Editors: Yuping Wu, Keyu Xie **Copy Editor:** Jia-Xin Zhang **Production Editor:** Jia-Xin Zhang

Abstract

Conventional lithium-ion batteries with inflammable organic liquid electrolytes are required to make a breakthrough regarding their bottlenecks of energy density and safety, as demanded by the ever-increasing development of electric vehicles and grids. In this context, solid-state lithium batteries (SSLBs), which replace liquid electrolytes with solid counterparts, have become a popular research topic due to their excellent potential in the realization of improved energy density and safety. However, in practice, the energy density of SSLBs is limited by the cathode mass loading, electrolyte thickness and anode stability. Moreover, the crucial interfacial issues related to the rigid and heterogeneous solid-solid contacts between the electrolytes and electrodes, including inhomogeneous local potential distributions, sluggish ion transport, side reactions, space charge barriers and stability degradation, severely deteriorate the cycle life of SSLBs. Solidification, which converts a liquid into a solid inside a solid battery, represents a powerful tool to overcome the aforementioned obstacles. The liquid precursors fully wet the interfaces and infiltrate the electrodes, followed by in-situ conformal solidification under certain conditions for the all-in-one construction of cells with highly conducting, closely contacted and sustainable electrode/electrolyte interfaces, thereby enabling high energy density and long cycle life. Therefore, in this review, we address the research progress regarding the latest strategies toward the solidification of the electrolyte layers and the interfaces between the electrodes and electrolytes. The critical challenges and future research directions are proposed for the solidification strategies in SSLBs from both science and engineering perspectives.

Keywords: Solid-state lithium batteries (SSLBs), solid electrolytes, interfaces, solidification, high energy density, long cycle life



© The Author(s) 2022. **Open Access** This article is licensed under a Creative Commons Attribution 4.0 International License (<https://creativecommons.org/licenses/by/4.0/>), which permits unrestricted use, sharing, adaptation, distribution and reproduction in any medium or format, for any purpose, even commercially, as long as you give appropriate credit to the original author(s) and the source, provide a link to the Creative Commons license, and indicate if changes were made.



INTRODUCTION

The development of electric vehicles and grids has resulted in a high demand for secondary batteries with markedly increased energy density and safety^[1-3]. Conventional lithium-ion batteries consisting of combustible organic liquid electrolytes and graphite anodes have nearly reached their upper limit of energy density^[4,5]. Furthermore, the leakage, thermal runaway and explosions related to organic liquid electrolytes have led to safety hazards^[2,5,6]. Concerning the improvement of energy density, Li metal, with the highest theoretical specific capacity of 3860 mAh g⁻¹ and the lowest reduction potential of -3.04 V versus a standard hydrogen electrode among metal anodes, should be the ideal anode^[7-9]. However, the usage of Li-metal anodes usually causes a gradual performance degradation resulting from the continuous side reactions between the liquid electrolytes and active Li metal and the consequent dendrite growth that may penetrate the separator, resulting in an internal short circuit^[10,11]. In this context, solid-state lithium batteries (SSLBs) have received significant attention due to their potential for solving these safety problems by replacing the liquid electrolyte with a nonflammable solid counterpart^[12,13]. Solid electrolytes with a high modulus are expected to suppress dendrite growth and penetration. In addition, the stability of solid electrolytes enables the combination of high-voltage cathodes with Li-metal anodes. The lamination configuration allows for a bipolar structure and highly stacked unit cells. All these features are beneficial for enhancing energy density.

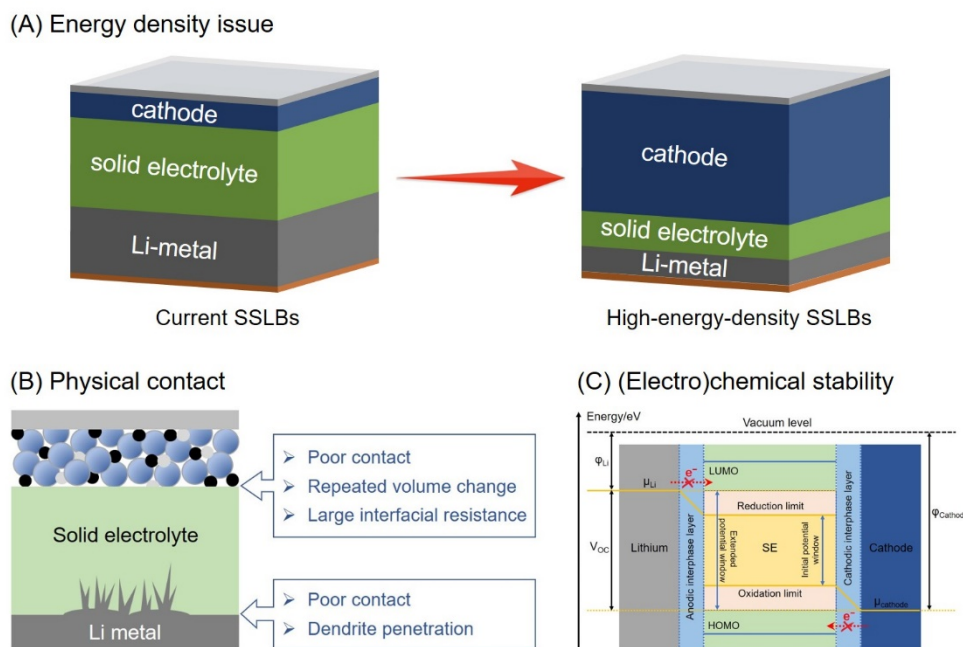
With respect to the aforementioned issues, here, we first discuss the difficulties in achieving high energy density regarding the cathodes, electrolyte layers and Li anodes, and those for obtaining long-cycle life regarding the interfaces. We then address solidification as a powerful tool for overcoming these difficulties. In the following section, the reported solidification strategies are summarized and the specific methods with respect to individual parts with different compositions are discussed in detail. The all-in-one solidification of SSLBs is pointed out as a useful means for building high-performance interfaces. The final section of this review presents the conclusions and perspectives for future directions.

SOLIDIFICATION TO OVERCOME THE LIMITS OF ENERGY DENSITY AND CYCLE LIFE OF SSLBS

Generally, although SSLBs theoretically exhibit the capability to have markedly improved energy density and safety, the most reported SSLBs deliver an energy density far below the required application level at present^[14]. Furthermore, the limited cycling and rate performance, i.e., generally lower than 500 cycles and 2 C^[14-17], respectively, of almost all existing solid battery systems also indicate that SSLBs are far from practical applications. Here, we address the key factors that constrain the energy density and cycling performance of SSLBs with respect to cathodes with a high mass loading, thin solid electrolytes, safe and stable anodes and sustainable electrode/electrolyte interfaces.

Difficulties in achieving high energy density

Although SSLBs have the advantages of coupling high-voltage cathodes with Li-metal anodes, tight stacking and simplified packaging, the achievement of high energy density remains challenging, which is mainly derived from the aspects of cathodes, solid electrolytes and Li anodes, as shown in [Scheme 1A](#). Generally, the expansion of cathode mass loading or thickness is limited by the sluggish kinetics of ion transfer in solid phases. Considering the mechanical strength and dendrite penetration of thin electrolytes, the thinning of electrolyte layers is difficult for both ceramic and polymer electrolytes. In addition, excess Li is always applied in solid batteries because Li metal shows a large volume variation during repeated plating/stripping cycles, likely leading to mechanical pulverization once the thin Li foil is used. The difficulties of the mass loading/thickness increase of the cathode, as well as the thickness decrease of the electrolyte and Li anodes restrict the high energy density of SSLBs.



Scheme 1. (A) Difficulties in achieving SSLBs with high energy density. (B) Physical contact and (C) (electro)chemical stability issues at multiscale interfaces inside SSLBs. SSLBs: Solid-state lithium batteries.

Cathodes

The energy density of a battery is influenced by the thickness or weight of its cathode, anode and electrolyte, as well as the additives, current collectors and even packaging. The cathodes are the active materials and their mass loading determines the available energy density. In contrast, the non-active components reduce the energy density at the cell level. Therefore, the design of the cathode plays a critical role in developing batteries with high energy density. Concerning SSLBs, on the cathode side, unlike liquid electrolytes that naturally wet porous cathodes and maintain good contact with the solid components during cycling, nonflowing solid electrolytes conventionally have poor contact with cathodes, especially concerning the volume change during cycling^[18,19]. This may block the transport of charge carriers. As a result, cathodes with a rather low mass loading or small thickness have been adopted in most reported SSLBs in order to access the satisfactory specific capacity during cycles^[14,20,21]. This unavoidably results in low energy density in the case of real SSLBs.

Given that the areal mass loading of the cathode strongly determines the delivered energy density, the construction of a thick cathode or a cathode with a high mass loading would maximally reduce the relative mass or volume of inactive components, which is pivotal for improving the energy density. Here, we propose an assumptive solid battery model consisting of a $\text{LiNi}_{0.8}\text{Co}_{0.1}\text{Mn}_{0.1}\text{O}_2$ (NCM) or LiFePO_4 (LFP) cathode and a Li anode to reveal the correlation between the cathode mass loading and energy density. According to the approximate calculations displayed in Figure 1A and B, the gravimetric energy density for the NCM/Li pouch cell is increased from 210 to 400 Wh kg^{-1} and the volumetric energy density is increased from 440 to 960 Wh L^{-1} with the mass loading of NCM increasing from 10 to 40 mg cm^{-2} . For the LFP/Li pouch cell, the equivalent values are increased from 170 to 270 Wh kg^{-1} and from 310 to 520 Wh L^{-1} , respectively, with the mass loading of LFP increasing from 13 to 40 mg cm^{-2} . The above calculations are carried out based on the assumption of a fixed polyethylene oxide: $\text{Li}_7\text{La}_3\text{Zr}_2\text{O}_{12}$ (PEO:LLZO) composite electrolyte with a mass density of 1.6 g cm^{-3} and a thickness of 100 μm . Nevertheless, a high mass loading or

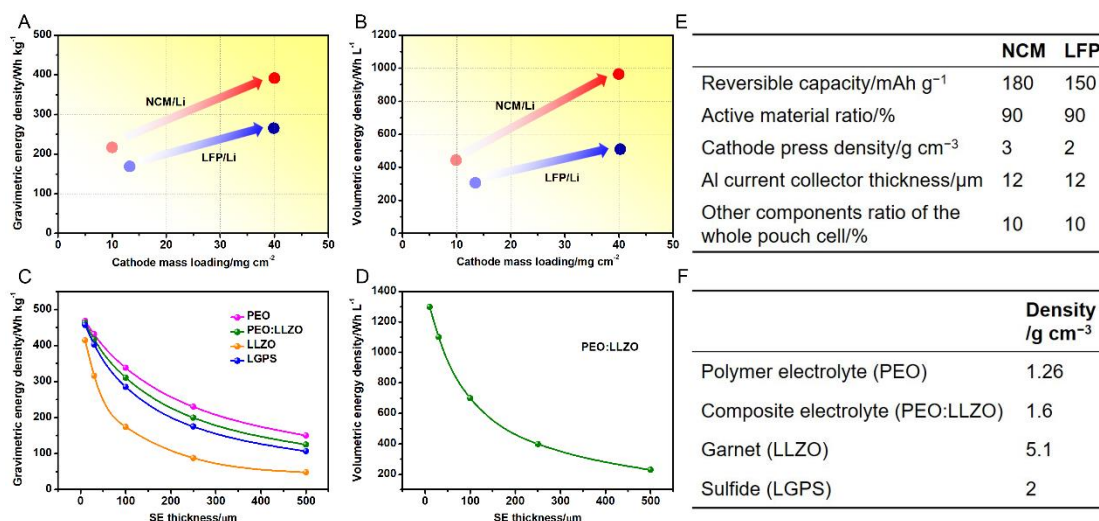


Figure 1. (A) Gravimetric and (B) volumetric energy density as a function of the mass loading of cathodes, which increases from 10 to 40 mg cm⁻² and from 13 to 40 mg cm⁻² for NCM/Li and LFP/Li pouch cells, respectively, with a fixed PEO:LLZO composite electrolyte with a mass density of 1.6 g cm⁻³ and thickness of 100 μm. (C) Gravimetric and (D) volumetric energy density as a function of electrolyte thickness, which is reduced from 500 to 10 μm for the NCM/Li pouch cell with a fixed cathode mass loading of 22 mg cm⁻². The corresponding calculation parameters are listed in (E) and (F), which are based on the battery operation temperature of 30 °C. NCM: LiNi_{0.8}Co_{0.1}Mn_{0.1}O₂; LFP: LiFePO₄; PEO:LLZO: polyethylene oxide:Li₇La₃Zr₂O₁₂.

thick cathode will limit its ion and electron transport efficiency. The ion transport near the current collector is relatively difficult, while a similar phenomenon occurs near the electrolyte for the electron transport. Therefore, the cathode configuration should be dedicatedly designed once a high mass loading or thick cathode is employed, including the construction of internal ionic and electronic conducting channels, external conducting pathways near the cathode boundaries and the amount and species optimization of the binders.

Electrolyte layers

To achieve SSLBs with high energy density, the construction of the electrolyte layers as thin as possible without sacrificing their functionality is also essential. Solid electrolytes can be classified into three types, namely, inorganic ceramic electrolytes, solid polymer electrolytes (SPEs) and composite polymer electrolytes (CPEs). Inorganic electrolytes, including oxides, oxynitrides and sulfides, are nonflammable, mechanically strong and thermally stable^[22-26]. However, they generally have a large mass density [e.g., 5.1 g cm⁻³ for Li₇La₃Zr₂O₁₂^[5], 2.92 g cm⁻³ for Li_{1+x}Al_xTi_{2-x}(PO₄)₃^[27], 2.4 g cm⁻³ for LiPON^[5] and 2.0 g cm⁻³ for Li₁₀GeP₂S₁₂(LGPS)^[4,28]], which makes it difficult to improve the gravimetric energy density of SSLBs at the cell level.

According to the calculation shown in [Figure 1C](#), the NCM/Li pouch cells based on the garnet LLZO and sulfide LGPS electrolytes deliver energy densities as low as 48 and 107 Wh kg⁻¹, respectively, assuming that each thickness is 500 μm. When reducing the electrolyte thickness from 500 to 10 μm, the gravimetric energy density for NCM/Li cell can reach higher than 410 Wh kg⁻¹, along with a greatly increased volumetric energy density of > 1300 Wh L⁻¹ [[Figure 1C and D](#)]. However, limited by the conventional sintering or cold pressing technique, the thickness of various ceramic pellets is difficult to reduce to < 500 μm, leading to a low energy density far below the application level^[14,29,30]. Furthermore, the reduced thickness is always accompanied with an increased risk of electrolyte fracture and even cell failure due to the brittle nature of inorganic ceramics. In contrast, SPEs consisting of polymer matrices with Li salts show the advantages of flexibility, lightweight, reduced thickness and easy mass production^[31-34]. In the case of CPEs,

inert (e.g., Al_2O_3 ^[35], SiO_2 ^[36] and TiO_2 ^[37]) or active fillers [e.g., $\text{Li}_{7-x}\text{La}_3\text{Zr}_{2-x}\text{Ta}_x\text{O}_{12}$ ^[38,39], $\text{Li}_{1.3}\text{Al}_{0.3}\text{Ti}_{1.7}(\text{PO}_4)_3$ ^[40] and $\text{Li}_{3x}\text{La}_{2/3x}\text{TiO}_3$ ^[41]] are further introduced into SPEs for increasing the ionic conductivity resulting from the decreased polymer crystallinity and/or generated percolation channels^[42]. Furthermore, the combination of rigid fillers with soft polymers reinforces the mechanical strength of CPEs, which contributes to Li dendrite suppression.

Under the assumption of the same electrolyte thickness ($\sim 500\ \mu\text{m}$) as the aforementioned inorganic ceramics, the energy densities of NCM/Li pouch cells with PEO and PEO:LLZO electrolytes are increased to 150 and 126 Wh kg^{-1} , respectively, which is ascribed to the low mass density of both SPEs and CPEs. Unlike inorganic solid electrolytes from powders to pellets that need sintering or cold pressing, SPEs and CPEs can be obtained by a tape-casting method, the thickness of which can be easily controlled to be less than 100 μm ^[30]. Therefore, the energy densities are estimated to be 337 and 311 Wh kg^{-1} and the corresponding volumetric energy density is 704 Wh L^{-1} for the NCM/Li pouch cells with PEO and PEO:LLZO electrolytes, respectively, with a thickness of 100 μm , as indicated in Figure 1C and D. All the aforementioned calculations are based on the parameters displayed in Figure 1E and F. It is clear that the further reduced thickness is accompanied by an obviously increased energy density for polymer electrolyte-based SSLBs [Figure 1C]. However, similar to inorganic ceramic electrolytes, the thinning of a polymer electrolyte also decreases its mechanical strength, leading to electrolyte fracture and dendrite penetration, both of which may cause final cell failure and safety hazards. Therefore, the challenges related to thin electrolyte designs are mainly concentrated on the consideration of both thickness minimization and electrochemical/mechanical performance sustainability.

Li anodes

Concerning the anode side, Li metal has been deemed as one of the most promising candidates for SSLBs due to its low mass density ($0.534\ \text{g cm}^{-3}$), high theoretical specific capacity ($3860\ \text{mAh g}^{-1}$) and ultralow reduction potential ($-3.04\ \text{V}$ versus a standard hydrogen electrode). However, the practical realization of SSLBs with high energy density still requires several obstacles to be overcome, including the Li excess, interfacial instability and dendrite growth. An applicable Li-metal battery calls for a thin Li-metal anode with an areal capacity below $4\ \text{mAh cm}^{-2}$ to couple with the common Li-based cathode^[43], which delivers an areal capacity of 3-4 mAh cm^{-2} at a practical level, i.e., the thickness of Li-metal foil should be less than 20 μm .

Nevertheless, Li-metal anodes display large volume variation during repeated plating/stripping cycles, which ultimately causes their mechanical pulverization^[44]. Such lithium pulverization severely damages the electrode continuity of the Li anode, cutting off the electrical contacts between the Li filaments and in between the solid electrolyte and the Li anode, thereby leading to rapid capacity and cycling efficiency fading. On this basis, an excessive amount of Li is often used in SSLBs to delay the occurrence of lithium pulverization and guarantee good cycling performance, even though it limits the cell-level energy density. Thus, pursuing a creative proposal to reduce the thickness of Li metal for increased energy density simultaneously without lithium pulverization is important. In addition, owing to the high reactive activity of Li metal, the interfacial stability between Li anodes and solid electrolytes (such as NASICON, perovskites, sulfides, halogenides and polymers) is also of significant concern. In addition, Li dendrite penetration across the solid electrolytes cannot be neglected, which seriously deteriorates the cycling life and safety of SSLBs. These critical interfacial issues related to the stability and safety of Li anodes are discussed in the following section.

Difficulties in achieving long cycle life

In addition to the energy density, the practical application of SSLBs is also challenged by their poor cycling and rate performance, which are strongly associated with crucial interfacial issues. These issues mainly refer to the physical contact and (electro)chemical stability at multiscale interfaces inside solid-state batteries, as shown in [Scheme 1B](#) and [C](#). Generally, the physical contact issue refers to the rigid and limited contact at electrode/electrolyte interfaces, along with the gradual contact loss during repeated cycling. The (electro)chemical stability issue refers to oxidation under high voltage on the cathodic side and reduction under low voltage on the anodic side, as well as the space-charge layer (SCL) effect induced by the deviation in chemical potentials between the solid components. These interfacial issues result in increased interfacial resistance and decreased interfacial stability, which account for the limited cycle life and battery safety.

Physical contact

In regard to physical contact, unlike fully infiltrated liquid-solid interfaces, the rigid and insufficient contacts between the various solid components in SSLBs lead to high interfacial resistance and thus large electric polarization. The volume changes induced by the phase transition from Li^+ intercalation/deintercalation, as well as the internal stress nonuniformity from uneven reactions, may distort the original interfaces, leading to gradual contact loss and a further increase in interfacial resistance^[1,45]. Specifically, on the cathode side, undesirable point contacts appear inside the cathodes and at the cathode/electrolyte interfaces due to the rigidity and illiquidity of solid electrolytes. Furthermore, the repeated volume changes during cycling aggravate the separation of solid-solid contacts between the solid electrolyte, carbon, binder and the active cathode material. Such a deficiency in physical contact results in a transport barrier for the carriers and the reduction of active material utilization, both of which cause the deterioration of the delivered capacity. On the anode side, though the Li metal presents good flexibility, its physical contact with the solid electrolyte is still far from satisfactory, especially in the case of the rigid ceramic electrolytes with an intrinsically lithiophobic nature. As discussed above, the repeated volume expansion and shrinkage of the Li anode during plating and stripping cycles ultimately cause the pulverization of the anode, consequently resulting in contact loss among Li filaments and between Li anodes and electrolytes. This causes the inhomogeneous distribution of the local potential and thus uneven Li^+ flux, thereby accelerating the formation of Li dendrites^[46-48].

(Electro)chemical stability

The chemical potentials of the cathode (μ_{cathode}) and Li anode (μ_{Li}) should be considered when referring to the interfacial (electro)chemical stability in SSLBs. If the μ_{cathode} and μ_{Li} are in the potential window of the solid electrolyte, the electrode/electrolyte interfaces are thermodynamically stable^[45,49]. Otherwise, (electro)chemical side reactions take place, including oxidation and reduction at the electrodes^[45,49]. The deviation in chemical potentials between the cathode and the electrolyte triggers the redistribution of charge carriers at the interface, leading to the SCL effect. If the SCL blocks ion transport, the high-resistance region will form, giving rise to the jumping of interfacial potential and the expansion of polarization. In addition, when in contact with high-voltage cathode materials, the oxidative decomposition of solid electrolytes at high operating voltages may accelerate the failure of the electrolyte. Zhu *et al.*^[50] and Nolan^[51] investigated the oxidative stability of various solid electrolytes through computation using the Materials Genome, such as initial oxidation potentials of ~ 2.0 to 2.5 V for sulfides and higher than 3 V for oxides.

In addition to the risk of oxidation at the cathodic side, many solid electrolytes, like $\text{Li}_{1+x}\text{Al}_x\text{Ti}_{2-x}(\text{PO}_4)_3$ (LATP)^[52], $\text{Li}_{3-x}\text{La}_{2/3-x}\text{TiO}_3$ (LLTO)^[53], LGPS^[54] and Li_3InCl_6 ^[55], which contain high-valence metallic elements, suffer from continuous reduction reactions when in direct contact with Li metal, given its strong reducibility and low potential. This leads to the formation of unstable Li/electrolyte interfaces with mixed ionic/electronic conductivity. Zhu *et al.*^[50] also studied the reduction stability for such types of solid

electrolytes through computation using the Materials Genome. For instance, LGPS started to be lithiated and reduced at 1.71 V with the decomposition products of Li_3P , Li_2S and $\text{Li}_{15}\text{Ge}_4$, while the reduction potentials of 1.75 and 2.16 V were calculated for oxide LLTO and LATP electrolytes, respectively. Comparatively, they further reported that LiPON compounds possessed a significantly lower reduction potential of 0.69 V with the reduction products of Li_3N , Li_2O and Li_3P against Li, and garnet LLZO showed the lowest reduction potential of 0.05 V, indicating its good kinetic stability against Li metal. Such electrochemical instability, together with the poor physical contact on the Li-anode side, further enables the generation of Li dendrites. Additionally, the residual electronic conductivity of solid electrolytes partially allows for electron transport, particularly at defect sites^[56]. Such electronic conductivity may induce the nucleation/growth of Li metal at defects, especially under the condition of high current density, also leading to dendrite penetration and short circuit^[56]. In brief, the physical contacts in combination with the (electro)chemical stability result in serious deteriorations in battery performance and safety.

Solidification as a solution for overcoming the difficulties facing SSLBs

Inspired by the ideal liquid-solid interfaces in conventional liquid batteries, the concept of “solidification” has been proposed for solid batteries, where the liquid precursor is in-situ transformed from high mobility to a (quasi)solid state inside the battery under mild thermal, light or electrical conditions. As shown in [Figure 2](#), the liquid precursor is injected at the electrode/electrolyte interface or between the cathode and the anode, followed by in-situ conversion into a (quasi)solid layer under certain conditions. Before solidification, the liquid precursor with high mobility can adequately fill the voids at the electrode/electrolyte interface and infiltrate the porous cathode. After solidification, the liquid is conformally immobilized at the filled sites, which not only guarantees continuous contact among the solid components for fluent charge transport, but also maximally maintains the solid-state of the batteries.

The solidification ensures the construction of ionic conducting channels and reinforces the interfacial compatibility throughout the whole battery, thereby enabling a high mass loading or thick cathode. The solid electrolytes synthesized by solidification can be easily controlled into a small thickness with less tendency of fracture in comparison with the self-supporting electrolytes prepared by conventional ex-situ methods. Furthermore, the contact of the Li/electrolyte interface can be simultaneously strengthened, which is beneficial for even Li plating and stripping, thereby realizing a highly stable anodic interface with a reduced possibility of dendrite growth. The dense packing of the solidified layer on the Li anode and the resultant even Li^+ flux improve the homogeneity of the Li anode, decreasing the risk of Li pulverization and enabling a thin Li anode. From this perspective, solidification contributes to the improvement of interfacial contact and the thickness optimization of each layer, which reveals significant potential in addressing the energy density and performance bottlenecks for solid batteries.

Until now, many solidification strategies have been developed to improve the densification of diverse interfaces in SSLBs, which can be approximately divided into two major categories, namely, physical and chemical solidification based on different solidifying mechanisms (as summarized in [Figure 3](#)). For physical solidification, only the states of certain components in SSLBs change among gas, liquid and solid with temperature variations, during which no chemical reactions take place. Physical solidification mainly involves “evaporation solidification” that evaporates the liquid solvent as a gas at high temperature to leave behind the solid component, and “heating-cooling solidification” that converts the electrolyte from the solid to liquid phase at high temperature and then turns back to the solid state during the cooling process. In contrast, chemical solidification refers to the processes involving (electro)chemical reactions, which induce the transformation from liquid precursors to solid phases inside the batteries. The typical polymerization from liquid monomers to solid polymer matrixes under moderate conditions, as well as the in-situ solid product formation induced by the electrochemical reactions between liquid additives and electrodes belong

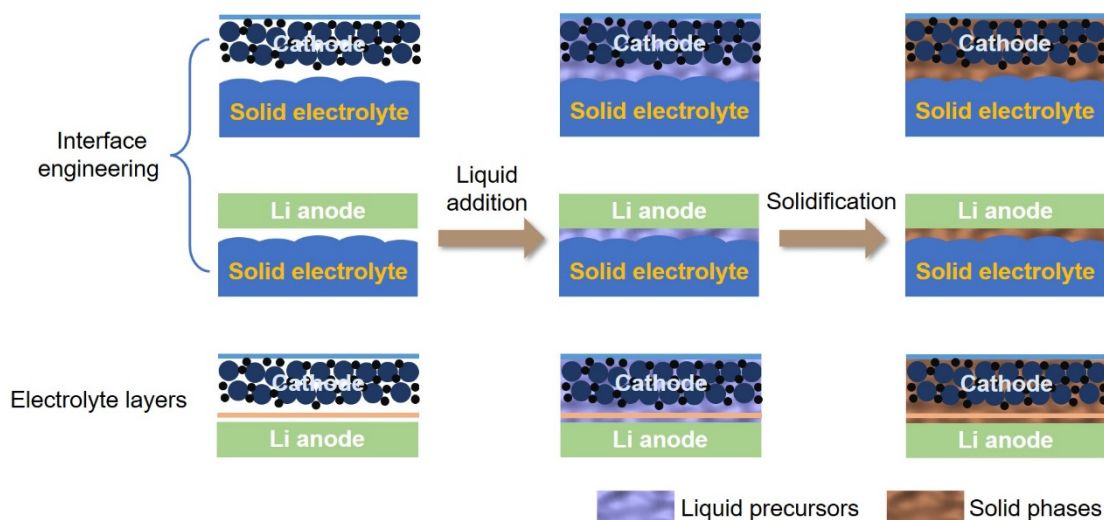


Figure 2. Process of solidification toward electrolyte layers and interfacial engineering on both the cathode and anode sides in SSLBs. SSLBs: Solid-state lithium batteries.

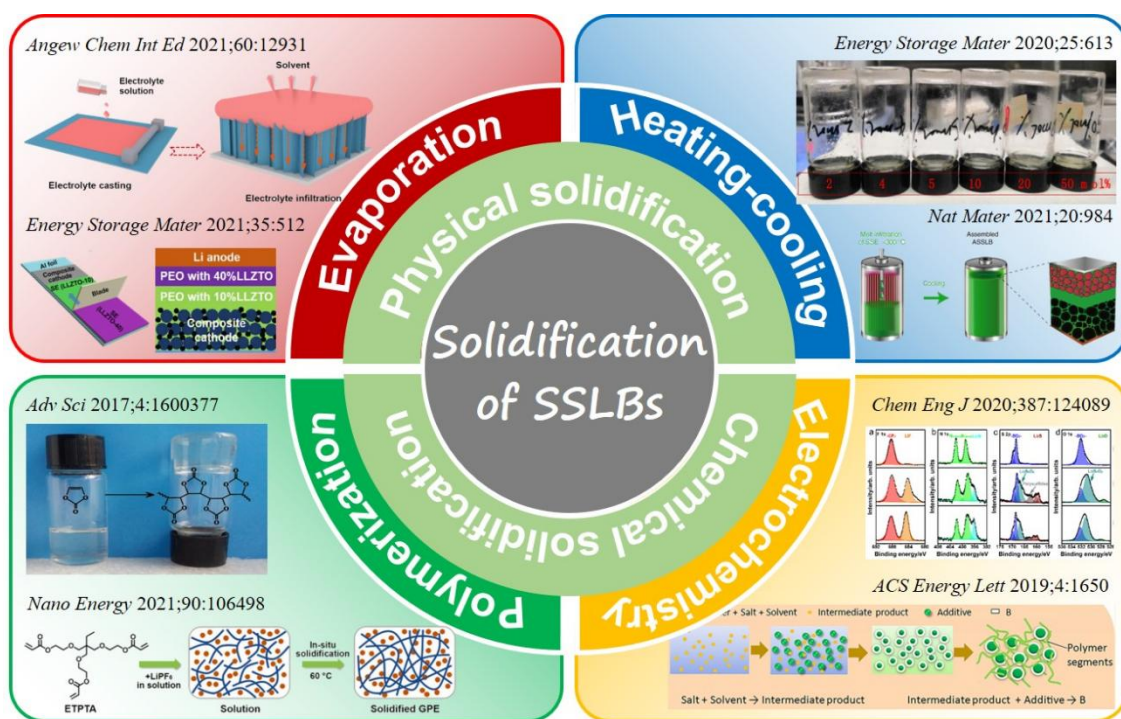


Figure 3. Summary of solidification strategies in SSLBs from the perspective of physical and chemical methods. Reproduced with permission from Ref.^[63] (Copyright 2021 Wiley-VCH GmbH), Ref.^[64] (Copyright 2020 Elsevier B.V.), Ref.^[111] (Copyright 2019 Elsevier B.V.), Ref.^[67] (Copyright 2021 Springer Nature), Ref.^[69] (Copyright 2016 WILEY-VCH Verlag GmbH & Co. KGaA, Weinheim), Ref.^[70] (Copyright 2021 Elsevier Ltd.), Ref.^[19] (Copyright 2020 Elsevier B.V.) and Ref.^[35] (Copyright 2019 American Chemical Society). SSLBs: Solid-state lithium batteries.

to the “chemical solidification” category. The solidification strategies according to different solidifying mechanisms are specifically discussed as follows.

(1) *Evaporation solidification*. Traditionally, ex-situ technologies, such as solid phase sintering, cold pressing and tape casting, have been widely used to prepare both self-supporting ceramic and polymer solid electrolytes^[8,57-61]. In this case, the cathodes, anodes and solid electrolytes are separately fabricated, leading to a mass of interfacial voids as a result of poor solid-solid contacts. The transport of Li ions and electrons is therefore affected, which is harmful to the battery performance. Overall, it is difficult to reduce the thickness of solid electrolytes through ex-situ technologies due to the dramatic decrease in mechanical strength for thin self-standing electrolytes. To minimize the interfacial mismatch, the structure of cathode-supported electrolytes formed by solvent evaporation has been proposed, for which the flowing electrolyte slurry is directly cast onto the cathode, followed by the electrolyte infiltration and solvent evaporation under high temperature^[62,63]. The realization of evaporation solidification is based on the difference between the volatilization temperature of the solvent and the melting points of the cathode components. The commonly used solvents for electrolyte slurries, such as N-methyl pyrrolidone^[38], acetonitrile^[40], dimethylformamide^[8,32] and acetone, are volatile and exhibit boiling points of < 200 °C, which are far below the melting points of cathode plates. The liquid electrolyte slurry can infiltrate into the voids inside the cathode and create good contact with it. During the high-temperature treatment, the solvent gradually evaporates, whereas all the cathode components are thermally stable. Therefore, after solvent evaporation, the solidified electrolyte fully occupies the voids between the cathode particles, accompanied by a greatly improved interfacial compatibility between the cathode and solid electrolyte, thereby rendering fluent Li⁺ diffusion. Moreover, benefitting from the support function of the cathode plate, the thickness of the solid electrolyte can be easily controlled to be less than 40 μm, thereby further increasing the practical energy density^[64].

(2) *Heating-cooling solidification*. Unlike evaporation solidification, no solvent participates in the “heating-cooling” solidification process. The solid electrolytes used here have low melting points (e.g., plastic crystals^[65,66] (~62 °C), anti-perovskites^[67] (~300 °C) and lithium metal halides^[68] (< 300 °C)) that are below those of cathodes and anodes. Such solid electrolytes exhibit a liquid state at temperatures higher than their melting point, while the cathode and anode remain in the solid state. When the temperature is decreased below the electrolyte melting point, the liquid electrolyte is gradually solidified between the cathode and the anode, leading to compact solid electrode/electrolyte contacts. With regards to succinonitrile (SN), its high polarity endows it with the capability to dissolve different types of Li salts, showing high ionic conductivity^[65,66]. In addition, it possesses a single plastic phase from -35 °C to the melting point of 62 °C^[65]. The “heating-cooling” process accounts for SN-based electrolytes from liquid to solid, the plasticity of which not only helps to make a flexible and seamless interfacial contact, but also accommodates the volume changes during the Li intercalation/deintercalation process. Similarly, other solid electrolytes with low melting points (below 300 °C), including anti-perovskites, lithium metal halides and lithium hydrides, are also compatible with the “heating-cooling” technology^[67]. These electrolytes can be adequately infiltrated into porous electrodes at moderate temperatures (below 300 °C) in a high-mobility state and then in-situ solidified inside the batteries during the cooling process. If the “heating-cooling” technology is matched with the temperature-resistant cathode and anode, the interfacial issues can be greatly ameliorated and the barrier for the SSLB industry will be reduced due to the availability of similar manufacturing facilities for commercial liquid batteries.

(3) *Polymerization solidification*. Conventional SPEs are generally prepared by tape-casting methods, i.e., polymers, Li salts and other fillers are uniformly dispersed in the solvent to form the precursor slurry, which is cast on the substrate, followed by completely volatilizing the solvent to obtain the self-supporting SPEs after peeling them off from the substrate. In addition to the interfacial issues resulting from the use of such SPEs, as discussed above, ex-situ casting is complicated and always associated with the consumption of large amounts of organic solvents, which is detrimental to the environment. In contrast, the in-situ membrane

formation technique^[69-73], which triggers the crosslinking or polymerization of monomers from the liquid to solid state inside the battery with or without the initiators under certain conditions, would realize a more conformal interface according to the natural morphology of the solid components. Polymerization generally refers to radical polymerization inside the batteries. The initiator molecules can produce radicals under thermal activation or photoactivation. For instance, the most common azobisisobutyronitrile (AIBN) initiator is divided into two radical fragments at $> 60\text{ }^{\circ}\text{C}$ or ultraviolet radiation^[74]. The reactive radical fragments, including carbo- or oxy-radicals, break and then activate the $\text{C} = \text{C}$ bonds of vinyl-containing compounds and acrylates or the $\text{C} = \text{O}$ bonds of aldehydes and ketones. Considering the non-transparency of batteries, thermal initiators rather than photoinitiators are suitable for in-situ polymerization^[74,75]. Furthermore, the polymerization can take place in the presence of lithium salts without impurities at milder conditions and even room temperature. Protonic or Lewis acids, like BF_3 and PF_5 , as the decomposition products of lithium salts, can induce the in-situ polymerization of cyanoethyl poly(vinyl alcohol), divinyl ethers and cyclic ethers without the introduction of an extra initiator^[74,75]. As a result, the solid particles can be tightly bonded by fulfilling the interspace using the in-situ generated SPEs, enabling smooth charge transport inside the entire battery. It is noteworthy that the in-situ membrane formation technique can be used in the fields of both interfacial engineering and solid electrolyte fabrication.

(4) *Electrochemistry solidification*. In order to stabilize the active materials and optimize the interfaces, coatings have proved to be a powerful means for interfacial engineering, especially in terms of SSLBs^[76]. Compared with conventional ex-situ coating methods by deposition or wet chemical techniques, the in-situ coatings derived from the interfacial reactions during cycling have excellent adhesive force and uniform distribution on solid particle surfaces. If the specific liquid phases are introduced at electrode/electrolyte interfaces, the (electro)chemical reactions that preferably convert the liquid into a solid phase take place during battery cycling. The solid phases are generally known as solid electrolyte interphases (SEI) at the anodic interface and cathode electrolyte interphases (CEI) at the cathodic interface. As a result, the ratio of liquid to solid phase can be effectively decreased depending on the degree of liquid-to-solid conversion. The desirable products derived from the in-situ interfacial reactions are conformally coated on solid particle surfaces, which strengthen the interaction between electrodes and electrolytes for intimate contact and even Li^+ transfer and long-term stability^[76]. These (electro)chemical reactions between electrodes and liquids are determined by the highest occupied molecular orbital (HOMO) and the lowest unoccupied molecular orbital (LUMO) energy levels of the additives in liquid phases^[77-79]. The ion with low LUMO energy level has a high electron-acceptance ability, which is prone to be reduced to form the SEI at the anodic interface, while the ion with high HOMO energy level possesses a high electron-donating nature, which is prone to be oxidized forming the CEI at the cathodic interface^[78]. This category of self-sacrificial additives^[18,35,80,81] mainly includes lithium bis(trifluoromethanesulfon)imide anion (LiTFSI), lithium bis(fluorosulfonyl)imide anion (LiFSI), lithium difluoro(oxalato)borate (LiDFOB), lithium bis(oxalate)borate, lithium fluoromalonato(difluoro)borate, tris(pentafluorophenyl)phosphine, methylene methanedisulfonate, tributyl borate and ionic liquids. In-situ electrochemically formed CEI/SEI layers are always composed of both inorganics (e.g., LiF , Li_3N , Li_2O and Li_2S from Li-salt additives) and organics (e.g., ROLi , ROCO_2Li and RCOO_2Li from organic solvent additives). Accordingly, the key is to design the CEI/SEI layer as a stable ionic conductor for fluent ionic transport with decreased resistance, as well as a good electronic insulator to avoid further corrosion. Nonetheless, since the reactions inside batteries are complicated and invisible, strategies to regulate interfacial reactions are still being explored and are severely challenged by preventing the undesirable reactions to acquire a stable interlayer during repeated charge/discharge cycling.

With the aim of achieving different application scenarios, a specific solidification strategy should be adopted. In the following section, the specific solidification strategies are reviewed regarding four aspects,

namely, cathodes, anodes, electrolyte layers and other new types of all-in-one solid batteries.

SOLIDIFICATION OF CATHODES

Porous cathodes consist of active cathode materials, conductive carbons and binders, which contain a significant number of voids even after being tightly pressed. This factor restricts the application of a high cathode mass loading or a thick cathode due to the poor solid-solid contact and lack of ionic conducting networks inside the cathode. Furthermore, the limited point contact between the cathode plate and the solid electrolyte and the SCL effect caused by the abrupt drop of electric potential across the cathode/electrolyte interface enlarge the interfacial resistance and polarization, leading to poor ion transport behavior and cycling performance. In order to implement a breakthrough in energy density and cycle performance, various solidification strategies have been developed with the aim of building conformal interfaces inside the cathode, as well as in between the cathode and the electrolyte. In this section, the designs and applications for the distinct solidification strategies are discussed in terms of different cathode materials, including LFP, LiCoO₂ (LCO) and NCM.

LiFePO₄

LiFePO₄ is a typical low-voltage cathode material with a charging potential within 4 V, leading to its high (electro)chemical stability with most solid electrolytes. Therefore, the focus on solidification for LFP is to improve the physical contact inside it and between it and the solid electrolytes. As the most widely used polymer electrolyte, PEO has attracted extensive attention in both fundamental research and practical applications due to its low cost and density and good film-forming ability^[82-85]. The low initial decomposition potential of PEO (~3.8 V vs. Li/Li⁺) gives it good compatibility with the low-voltage LFP cathode. To improve the physical contact of an LFP cathode with a PEO electrolyte, Chen *et al.*^[86] directly infused the flowing PEO electrolyte slurry into the porous cathode to form a cathode-supported solid electrolyte framework after solvent evaporation. The SSLB could be assembled by coupling the cathode-supported electrolyte with a Li-metal anode rather than stacking the separate cathode, electrolyte and anode together [Figure 4A]. On this basis, the interface between the LFP cathode and the PEO electrolyte was highly improved since the PEO slurry was filled into the voids of the cathode, followed by evaporation, leading to the formation of an ionic conductive network inside the cathode and intimate cathode/electrolyte contact. In addition, the cathode layer served as the support for the PEO electrolyte, thereby enabling a reduced electrolyte thickness of < 10 μm [Figure 4B].

Furthermore, Bi *et al.*^[64] designed a gradient PEO electrolyte through the solvent evaporation strategy, where PEO slurries with various LLZO filler contents were successively cast onto the cathode layer. The PEO-rich side with high ionic conductivity was in contact with the LFP cathode, which used the same PEO electrolyte instead of the common polyvinylidene difluoride (PVDF) as the binder, thereby greatly increasing the interfacial compatibility and stability. Furthermore, the LLZO-rich side with high mechanical strength was in contact with the Li-metal anode, which was beneficial for dendrite suppression and battery safety. As a result, a satisfying discharge capacity of 118 mAh g⁻¹ was delivered with a high cathode mass loading of 15.2 mg cm⁻². Considering the balance of electrolyte thickness and dendrite penetration, Lin *et al.*^[87] introduced a robust porous PVDF fiber network on the LFP cathode by electrospinning, after which the liquid PEO electrolyte precursor was infused into the PVDF network and the solvent was then removed to obtain an integrated cathode/electrolyte structure [Figure 4C]. Because of the reinforcing function of the robust PVDF fiber, an ultrathin electrolyte layer of 17 μm in thickness was achieved with high mechanical strength for dendrite inhibition.

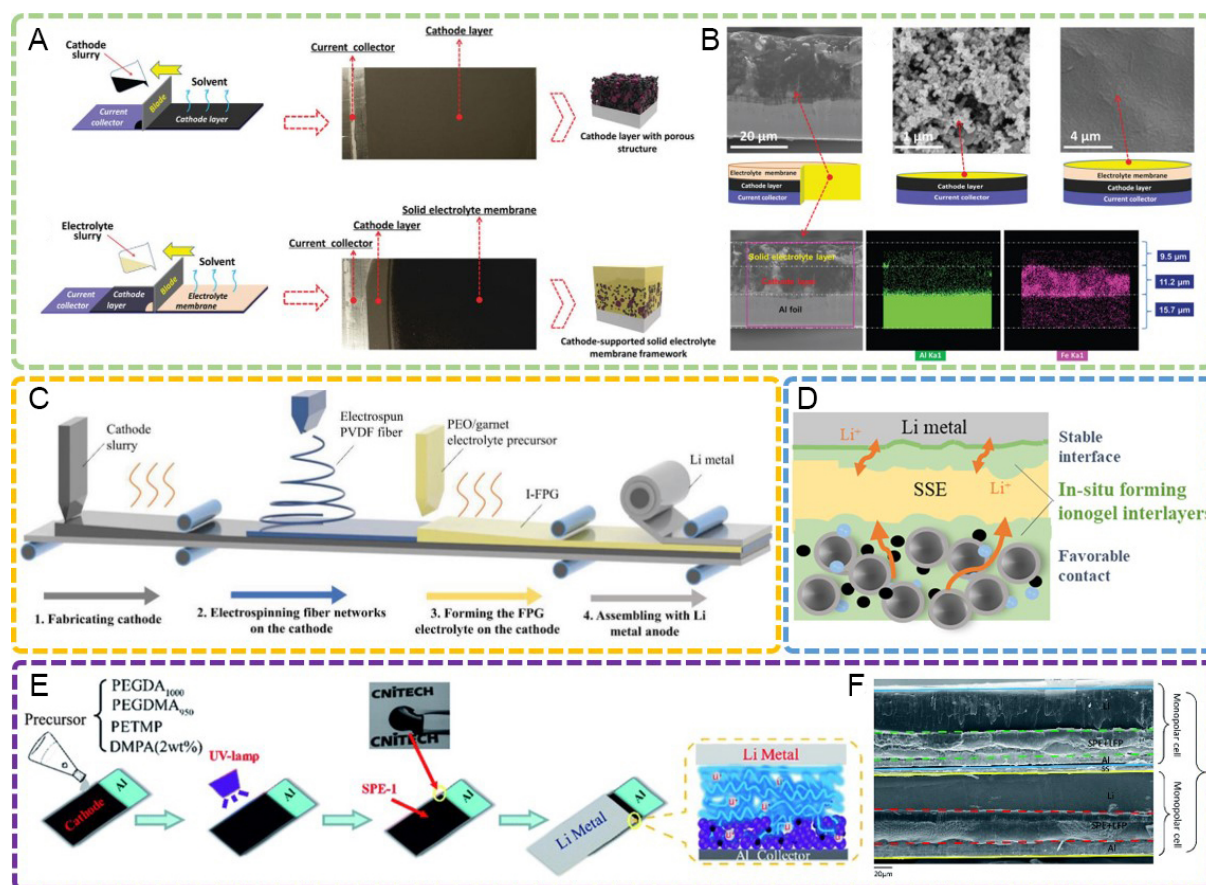


Figure 4. (A) Preparation of cathode-supported solid electrolyte framework by successive tape casting of the cathode and electrolyte slurry^[86]. Reproduced from Ref.^[86] with permission. Copyright 2019 Royal Society of Chemistry. (B) Cross-sectional morphology of cathode-supported structure, surface morphology of cathode layer and cathode-supported structure and elemental mapping in cross-sectional cathode-supported structure^[86]. Reproduced from Ref.^[86] with permission. Copyright 2019 Royal Society of Chemistry. (C) Schematic diagram of the fabrication process of solid battery with an integrated cathode/fiber-reinforced PEO/garnet electrolyte^[87]. Reproduced from Ref.^[87] with permission. Copyright 2021 Wiley-VCH GmbH. (D) Schematic diagram of the improved interface through in-situ formed ionogel interlayers^[88]. Reproduced from Ref.^[88] with permission. Copyright 2020 American Chemical Society. (E) Procedure and schematic structure for integrating an LFP cathode layer with in-situ polymerized solid electrolytes^[89]. Reproduced from Ref.^[89] with permission. Copyright 2018 Royal Society of Chemistry. (F) The battery in (E) can be assembled into a bipolar structure^[89]. Reproduced from Ref.^[89] with permission. Copyright 2018 Royal Society of Chemistry. PEO: polyethylene oxide; LFP: LiFePO_4 .

In addition to solvent evaporation, in-situ polymerization is also widely adopted in the solidification of LFP cathodes. Lin *et al.*^[88] fabricated an ionogel interlayer in an LFP/LATP interface via the in-situ thermal polymerization of poly(ethylene glycol) diacrylate (PEGDA) monomers with a $\text{Pyr}_{13}\text{TFSI}$ ionic liquid, Li-salt and AIBN initiator [Figure 4D]. The elastic crosslinked PEGDA/ $\text{Pyr}_{13}\text{TFSI}$ ionogel interlayer was in-situ solidified at the cathodic interface, resulting in reduced interfacial resistance and long-term cycling. By taking advantage of the decreased electrolyte thickness and integrated battery structure resulting from the in-situ polymerization, bipolar and even multipolar cells could be assembled by directly stacking isolated monopolar cells layer by layer, leading to an increased output voltage and accordingly a higher energy density. As shown in Figure 4E and F, Wei *et al.*^[89,90] developed a bipolar battery by integrating an LFP cathode with an ultraviolet polymerized polycarbonate electrolyte, whose open-circuit voltage could be elevated to 6.07 V, leading to a wide output voltage and increased energy density.

LiCoO₂

The coupling of a Li-metal anode with a high-voltage cathode is a promising approach to expand the energy density of SSLBs. LCO is an important commercial cathode material with a high charging voltage of > 4 V. Therefore, with the objective of achieving interfacial optimization by solidification, the compatibility between LCO and solid electrolytes should be considered to prevent side reactions at cathodic interfaces.

Although PEO-based polymer electrolytes are stable against LFP cathodes, they suffer from oxidative decomposition to release gas at potentials of >3.8 V (vs. Li/Li⁺) due to the severe dehydrogenation process. Nie *et al.*^[91] further reported that high-voltage LCO promotes such PEO degradation as a result of the surface chemical activation for PEO dehydrogenation. In view of this, various in-situ polymerized polymers, such as poly(vinylene carbonate) (PVCA)^[92] and poly(ethyl cyanoacrylate)^[93], with the capability to withstand high voltages have been introduced as interlayers to improve the compactness, as well as the stability, of LCO/PEO interfaces [Figure 5A].

Given the high voltage-resistant nature of sulfides, Kim *et al.*^[94] reported a solvent evaporation strategy for LCO by infiltrating an ethanol solution of Li₆PS₅Cl (LPSCl) into the LCO cathode, followed by a heat treatment to evaporate the ethanol and cold pressing to densify the cathode layer [Figure 5B]. The wide electrochemical window of LPSCl enables its good compatibility with LCO, while the high ionic conductivity and mechanical ductility contribute to uniform Li⁺ interfacial transfer. Consequently, a high LCO mass loading of 10 mg cm⁻² was obtained, delivering a discharge capacity of 141 mAh g⁻¹ (charging from 3.0 to 4.2 V) at 30 °C.

Like the formation of CEI/SEI layers in liquid batteries^[95], the preferable (electro)chemical decomposition of a trace liquid electrolyte or ionic liquid into a solid phase can markedly strengthen the interaction between cathodes and electrolytes. Bi *et al.*^[19] proved that the anion group of the N-methyl-N-propylpiperidinium bis(trifluoromethanesulfonyl)imide (PP₁₃TFSI) ionic liquid can be decomposed into solid ionic conducting interphases of LiF and Li₃N at the LCO/garnet interface during cycling. This partial liquid-to-solid conversion reduced the ratio of liquid phases in the batteries and enhanced the ion transfer across the interface. Zhang *et al.*^[96] introduced the 1-methyl-1-propylpiperidinium tetrafluoroborate (PP₁₃BF₄) ionic liquid at the LCO/PEO interface. Compared with the bare LCO/PEO interface, the N-O bond was attributed to the decomposition product of the PP₁₃BF₄ additive. As PP₁₃BF₄ takes part in the formation of the protective CEI layer, the parasitic reactions between LCO and the PEO electrolyte can be effectively suppressed [Figure 5C].

By virtue of the low-temperature solidification nature of SN, Feng *et al.*^[97] cast liquid SN on an LCO surface at 70 °C, followed by conformal solidification during the cooling process [Figure 5D]. The SN-modified LCO cathode was coupled with the in-situ ring-opening polymerized 1,3-dioxolane (DOL) solid electrolyte, resulting in a high LCO loading of 7 mg cm⁻², benefitting from both the optimized cathodic and anodic interfaces. In addition to SN, the high ionic conducting lithium-rich anti-perovskite electrolyte also exhibits a relatively low melting point of 273.2 °C. Chen *et al.*^[98] made use of its low melting point to in-situ coat an LCO cathode to obtain an intimate LCO/LATP contact and continuous ionic conducting network [Figure 5E]. The highest temperature during battery fabrication was controlled below 290 °C, which effectively restricted both Li⁺/H⁺ exchange and interdiffusion phases. Furthermore, the good ductility of the anti-perovskite led to restricted contact failure and prolonged cycling.

LiNi_{1-x-y}Co_xMn_yO₂

NCM is a topical cathode material due to its high voltage and specific capacity. However, its high oxidability means that it is prone to causing side reactions at the NCM/electrolyte interface, leading to inferior ion

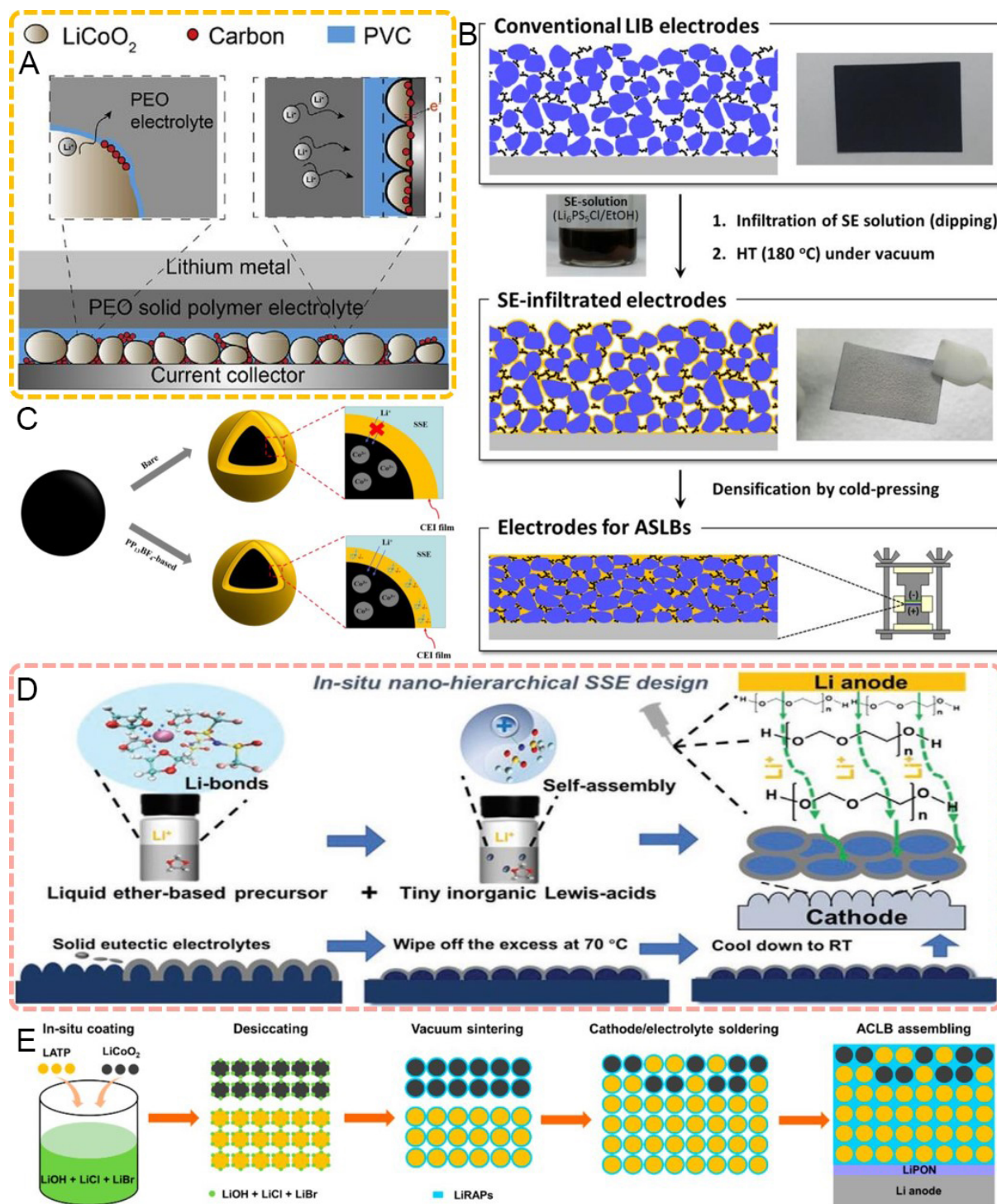


Figure 5. (A) Schematic diagram of in-situ polymerization for the stability of an LCO/PEO interface^[92]. Reproduced from Ref.^[92] with permission. Copyright 2020 Elsevier B.V. (B) Schematic diagram of LCO electrode layer after infiltration of LPSCl and cold pressing^[94]. Reproduced from Ref.^[94] with permission. Copyright 2017 American Chemical Society. (C) Role of $\text{PP}_{13}\text{BF}_4$ ionic liquid on the formation of protective CEI on LCO surface^[96]. Reproduced from Ref.^[96] with permission. Copyright 2020 Elsevier Ltd. (D) SN-modified LCO cathode coupled with in-situ polymerized solid electrolyte^[97]. Reproduced from Ref.^[97] with permission. Copyright 2021 Wiley-VCH GmbH. (E) Ionic conducting network inside LCO cathode by heating and cooling a lithium-rich anti-perovskite solder^[98]. Reproduced from Ref.^[98] with permission. Copyright 2021 American Chemical Society. LCO: LiCoO_2 ; PEO: polyethylene oxide; LPSCl: $\text{Li}_6\text{PS}_5\text{Cl}$; CEI: cathode electrolyte interphases.

transfer and cycling stability. To mitigate these issues, it is effective to introduce high-voltage groups, such as $-C \equiv N$, in solid electrolytes or construct artificial CEIs by coating NCM cathodes with desirable compounds.

Polyacrylonitrile (PAN) shows high stability when in contact with a high-voltage cathode due to the oxidation-resistant group of $-C \equiv N$. Qiu *et al.*^[99] constructed a PAN layer at a $\text{LiNi}_{0.5}\text{Co}_{0.2}\text{Mn}_{0.3}\text{O}_2$ cathode surface to stabilize the NCM/PEO interface. The PAN layer was formed by electrically polymerizing an acrylonitrile (AN) monomer with a LiDFOB salt [Figure 6A], which isolated the direct contact of NCM and the PEO electrolyte. Consequently, a satisfactory capacity retention of 72.3% was acquired, even after 200 cycles at 3.0-4.2 V. To address the NCM/garnet interfacial issues, Huang *et al.*^[100] introduced trace a 1-butyl-3-methylimidazolium bis(trifluoromethylsulfonyl)imide [(bmim)(Tf₂N)] ionic liquid in between the NCM cathode and garnet electrolyte. As shown by the X-ray photoelectron spectra in Figure 6B, the ionic liquid could partially be converted into solid ionic conducting phases of LiF and Li₃N at the NCM/garnet interface during cycling. The residual ionic liquid and solid products at the NCM/garnet interface led to reduced interfacial resistance and improved Li⁺ conduction. The further addition of distinct salts in the SPE can promote the electrolyte stability and help to build a functional CEI layer for a robust NCM/electrolyte interface. Zhao *et al.*^[101] prepared an ether-based solid electrolyte by the in-situ ring-opening polymerization of DOL with the addition of AlF₃ [Figure 6C]. On the one hand, the introduction of AlF₃ to the poly-DOL electrolyte created a solution with saturated Al³⁺ and immobilized TFSI. This inhibits the dissolution of Al₂O₃ from the current collector, thereby effectively protecting the current collector. On the other hand, the AlF₃ participated in the formation of LiF in the CEI layer, thereby enhancing the oxidative stability of the electrolyte solvents. The synergetic in-situ polymerization and CEI design enabled a solid NCM/Li battery with a high specific capacity of 153 mAh g⁻¹ at a large areal capacity of 3.0 mAh cm⁻².

SOLIDIFICATION OF LI ANODES

Since Li metal possesses a high reactive activity and low reduction potential, both the compact contact between the solid electrolyte and the Li anode for even Li plating/stripping and the inhibition of the solid electrolyte reduced by Li for a stable anodic interface should be taken into consideration regarding solidification on the anode side. Furthermore, due to the local electric field concentration and the electron injection that leads to the inevitable growth of Li dendrites, the solidification should also concern the electric field homogeneity and electron blocking at the Li/electrolyte interface.

When the NASICON-type solid electrolyte $\text{Li}_{1-x}\text{Al}_x\text{M}_{2-x}^{3+4+}(\text{PO}_4)_3$ ($M = \text{Al}$ or Ge) is in contact with Li, the high-valence M ions tend to be continuously reduced from M^{4+} to M^{3+} , inducing the formation of an interphase with decreased ionic conductivity and the rapid failure of solid batteries. Zhang *et al.*^[102] designed a bifunctional in-situ generated PVCA-based buffer layer between a $\text{Li}_{1.5}\text{Al}_{0.5}\text{Ge}_{1.5}(\text{PO}_4)_3$ (LAGP) electrolyte and a Li anode [Figure 7A]. The in-situ solidified PVCA cuts off the direct contact of LAGP and Li, leading to an improvement in interfacial stability, while the compact interfacial contact was also guaranteed for the realization of dendrite-free Li plating/stripping. Zeng *et al.*^[103] and Duan *et al.*^[104] added ductile PEO into the liquid precursor in advance of the solidification, which was anchored at the interconnected solidified network. The combination of the “rigid” and “soft” natures of the solid electrolyte enabled both a low-resistance interface and dendrite suppression. In addition to functional polymer additives, Chai *et al.*^[105] added a γ -methyl-propylene trimethoxysilane (KH570)-modified garnet LLZO filler into vinylene carbonate (VC) monomers to form a three-dimensional (3D) crosslinked network after the polymerization process, which served as a “flexible-rigid” coupling skeleton to tolerate volume changes and suppress dendrite growth during cycling. The strong coordination interaction with Li⁺ offered by the C = O group in PVCA facilitated even ionic diffusion, while the rigid garnet filler could block dendrite propagation. This strategy

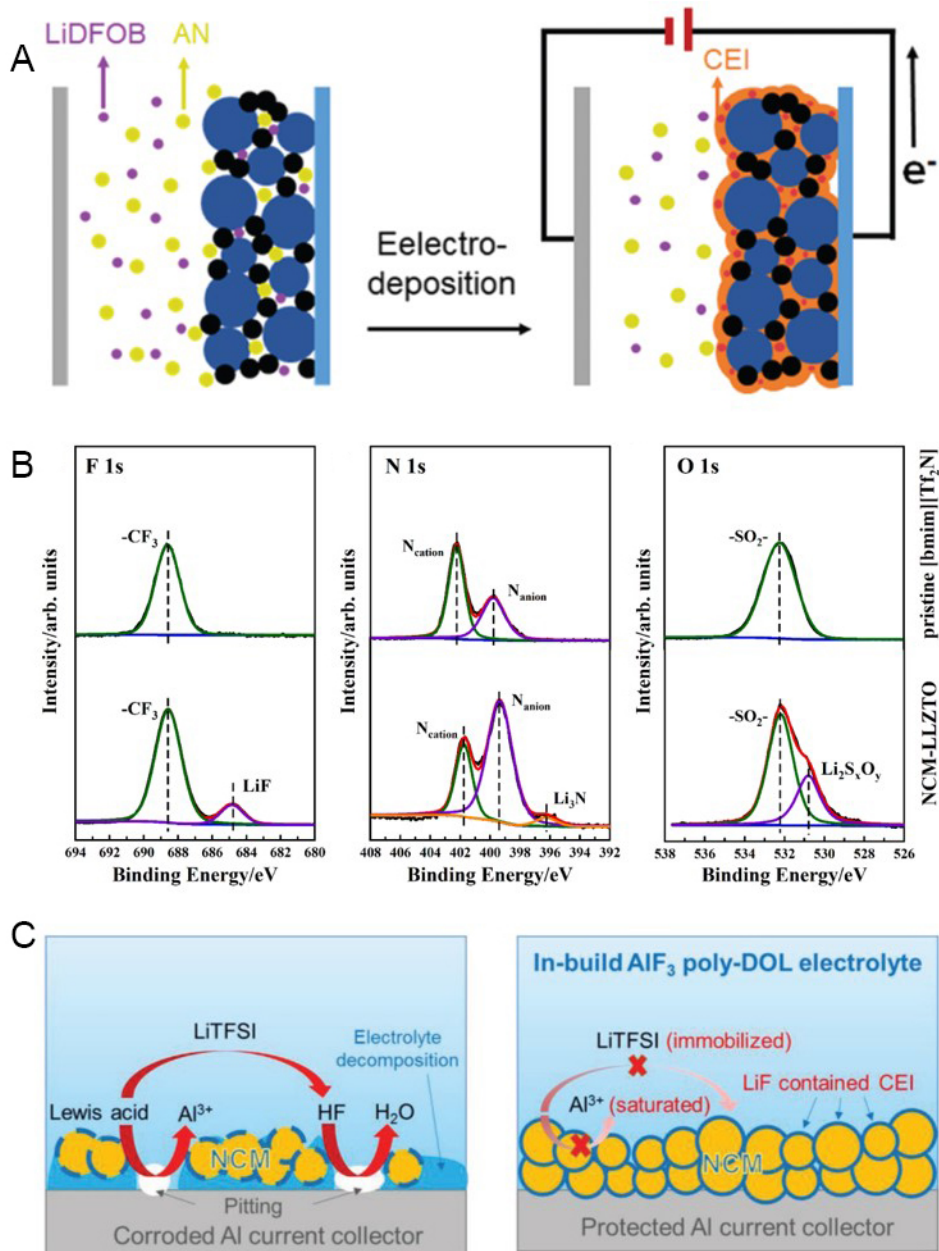


Figure 6. (A) Schematic diagram of electropolymerization of PAN-based coating layer on NCM cathode^[99]. Reproduced from Ref.^[99] with permission. Copyright 2020 Royal Society of Chemistry. (B) X-ray photoelectron spectra of pristine [bmim][Tf₂N] ionic liquid before cycling and NCM/garnet interface after cycling^[100]. Reproduced from Ref.^[100] with permission. Copyright 2021 Elsevier B.V. (C) Schematic diagram of Al current collector corrosion in routine electrolyte and AIF₃-poly-DOL electrolyte^[101]. Reproduced from Ref.^[101] with permission. Copyright 2020 WILEY-VCH Verlag GmbH & Co. KGaA, Weinheim. NCM: LiNi_{1-x-y}Co_xMn_yO₂

was highly compatible with a high-voltage LiNi_{0.5}Mn_{1.5}O₄ cathode (3.5 V -5.0 V) with an industrial mass loading of 18 mg cm⁻², revealing its significant potential in solid batteries with high energy density.

Artificial SEI construction has already been widely investigated in liquid-based lithium batteries^[95]. Various solvents and additives, including fluorides, fluoroethylene carbonate (FEC) and lithium nitrates, are conventional candidates for regulating interfacial reactions to obtain desirable interfacial compositions and

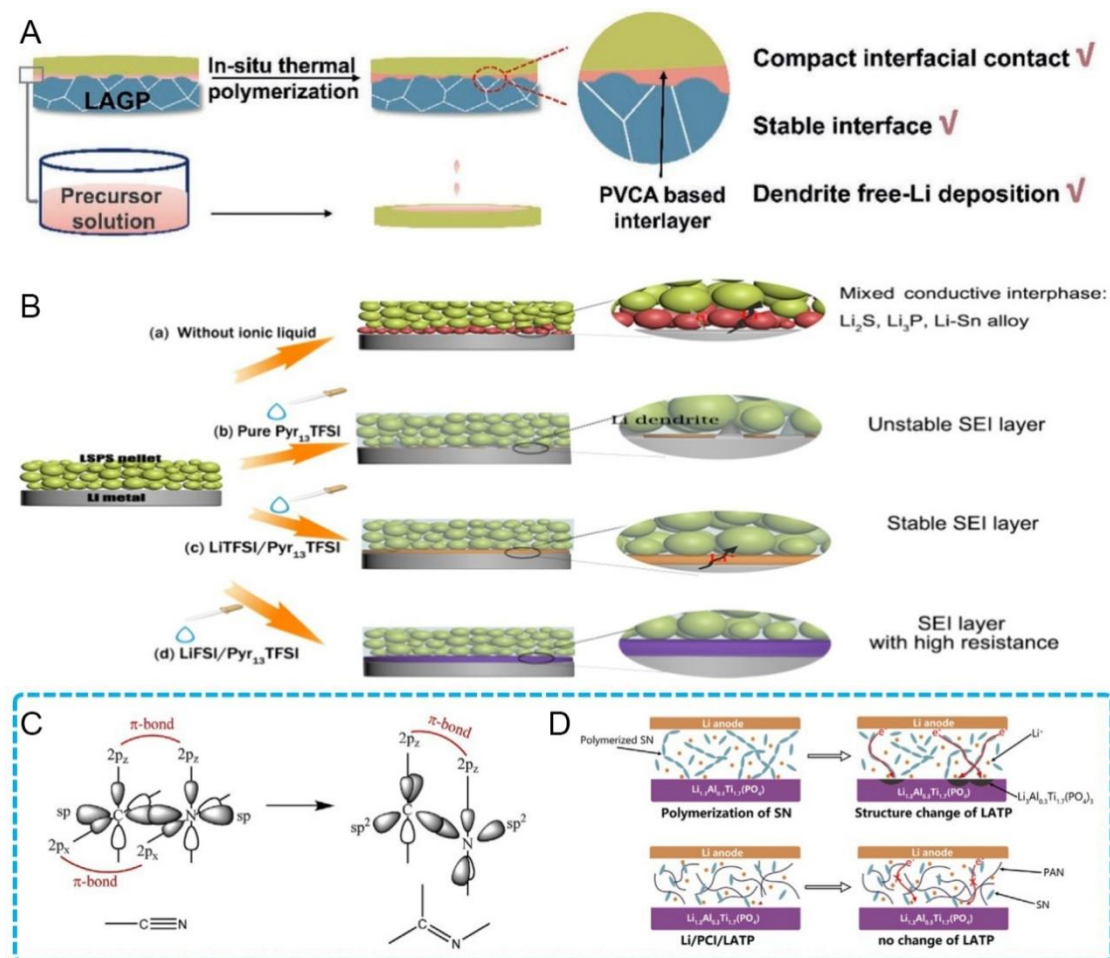


Figure 7. (A) Schematic diagram of in-situ polymerized PVCA-modified LAGP/Li interface^[102]. Reproduced from Ref.^[102] with permission. Copyright 2021 Wiley-VCH GmbH. (B) Schematic diagram of the formation of different SEIs for varying Li salt/Pyr₁₃TFSI at sulfide/Li interface^[107]. Reproduced from Ref.^[107] with permission. Copyright 2018 American Chemical Society. (C) Hybridization diagram of C and N atoms converting from sp into sp^2 and forming double bonds ($\sigma+\pi$) and conjugated structures^[110]. Reproduced from Ref.^[110] with permission. Copyright 2021 Elsevier Ltd. (D) Comparison of LAMP/Li interfaces with SN or SN/PAN composite layers^[110]. Reproduced from Ref.^[110] with permission. Copyright 2021 Elsevier Ltd. PAN: Polyacrylonitrile.

structures^[106]. Such artificial SEI design provides significant guidance for solid batteries. Huang *et al.*^[100] utilized a trace dual-salt ethylene glycol dimethyl ether electrolyte with LiTFSI and LiNO₃ to buffer the Li/garnet interface. A dual-layer SEI film with an inorganic-rich (Li₃N and LiF) inner layer and organic-rich (C-OR, C-C/C-H and lithium alkylcarbonate) outer layer was built at the Li/garnet interface through the in-situ decomposition of ether. The liquid ether electrolyte partially converted into a solid phase, thereby decreasing the liquid ratio in solid batteries and also realizing the combination of good flexibility and high mechanical strength. In order to ameliorate the instability of sulfides against Li, Zheng *et al.*^[107] used a Pyr₁₃TFSI-based ionic liquid as the interlayer to modify the Li₁₀SnP₂S₁₂ (LSPS)/Li interface and investigated the effects of different Li salt additives on the formation of SEI layers [Figure 7B]. A robust SEI containing a stable amount of LiF was in-situ formed through the conversion of LiTFSI/Pyr₁₃TFSI. It was also revealed that the LiFSI led to excessive LiF at the LSPS/Li interface with increased resistance, which was harmful to the cycling performance. Accordingly, the solidification strategy of regulating CEI/SEI components in solid batteries is still being explored. Previous studies have usually concentrated on inert interlayer formation to block the undesirable reactions between electrodes and solid electrolytes. Therefore, the methods for

constructing stable and ionic conducting CEI/SEI layers, as well as the interfacial chemistry, require further investigation.

Owing to the compatible melting points of SN (~62 °C) and Li (~180 °C), SN can be solidified on the Li surface through a “heating-cooling” process without breaking the solid state of Li during the SN liquation. Tong *et al.*^[108] mixed SN and LiTFSI as an intermediate layer in between LAGP and a Li anode to strengthen the interfacial compactness and restrict the reduction of LAGP by Li metal. However, the Li symmetric cell delivered cycles of less than 160 h, followed by continuously increasing polarization. This phenomenon can be attributed to the instability of SN against Li^[109,110]. The $-C \equiv N$ group in SN can be spontaneously polymerized into conjugated polymers by the catalysis of Li and the hybridization mode of adjacent C and N atoms in this polymer is transformed from sp into sp², as shown in Figure 7C^[110]. In addition, the delocalized π electrons in such a conjugated system can freely migrate and take part in the reduction of the NASICON-type $Li_{1-x}Al_x^{3+}M_{2-x}^{4+}(PO_4)_3$, leading to a deterioration in battery performance. The interfacial compatibility between the SN layer and Li can be improved by the introduction of functional additives, such as FEC^[111] and LiNO₃^[112], which have been proved to form protective SEI films at the Li surface. Cao *et al.*^[110] further studied the effect of a PAN additive on the stability of SN against Li [Figure 7D]. A plastic composite interlayer combining SN and PAN was introduced between LAGP and the Li anode. They proved that PAN served as a polymer skeleton that anchored the SN by strong C \equiv N dipole-pair bonds between the C \equiv N groups in both SN and PAN, which could avoid SN polymerization and prohibit electron transfer from the anode to electrolyte. The synergetic effect enabled the intimate interfacial contact by the “heating-cooling” process of SN and the high interfacial stability by anchoring SN in the PAN framework.

SOLIDIFICATION OF ELECTROLYTE LAYERS

The distinct solidification strategies toward different kinds of cathodes and Li anodes have been discussed, which result in reinforced electrode/electrolyte interfaces with good physical contact and high (electro)chemical stability. In addition, solidification can be further applied in the field of solid electrolyte fabrication for simultaneous interfacial optimization with both cathodes and Li anodes. Such solidification methods for in-situ generated solid electrolyte layers are highly compatible with the current fabrication process of liquid lithium-ion batteries, which facilitate the practical application of SSLBs.

In-situ polymerization initiated by radical reactions from a liquid to solid polymer under certain thermal, light or electrical conditions is typical for the in-situ generation of solid electrolytes^[74,113,114]. AIBN has been extensively used as a thermal initiator for the in-situ polymerization process. The radical reactions thermally induced by AIBN are easy to control with no byproducts. It has been manifested that polycarbonate-based polymer electrolytes with C = O bonds can afford fast ionic transfer pathways, which are beneficial for the improvement of ionic conductivity. Lin *et al.*^[115] designed a poly(vinyl ethylene carbonate) polymer electrolyte for an SSLB by in-situ thermal polymerization [Figure 8A]. The coupling/decoupling between Li⁺ and oxygen atoms in C = O/C-O groups, as well as the moving/exchange of Li⁺ between C = O and C-O groups in the process of segmental motions for high and low molecular polymers, contributed to the fast ionic transfer, achieving a superior ionic conductivity of ~2.1 mS cm⁻¹ at 25 °C. Furthermore, the interfacial compatibility could be significantly enhanced by such an in-situ solidification strategy compared with ex-situ generated polymer electrolytes.

Since 2017, the group of Cui has developed a series of in-situ polymerized SPEs based on VC. For instance, they constructed a PVCA electrolyte by polymerizing VC monomers and LiDFOB, as shown in Figure 8B^[69]. Li⁺ was prone to interact with the oxygen atom in PVCA, forming the Li⁺-O = C complex structure, which was beneficial for ionic transfer. In order to match with 5 V lithium batteries, they further designed a

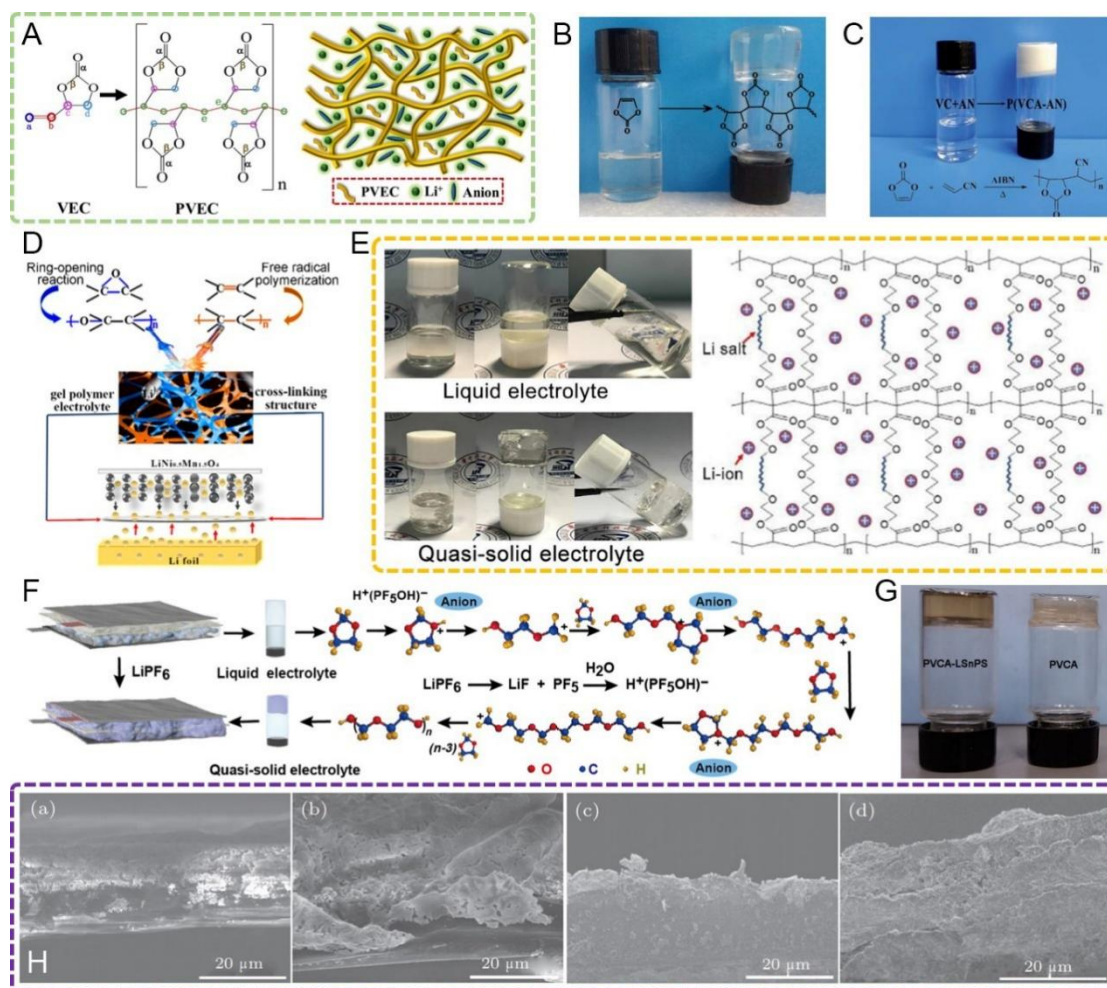


Figure 8. (A) Schematic diagram of poly(vinyl ethylene carbonate) with a chain structure polymerized from the vinyl ethylene carbonate precursor^[115]. Reproduced from Ref.^[115] with permission. Copyright 2020 Elsevier Ltd. (B) Photograph of polymerization from VC to PVCA after heating treatment at 60 °C for 24 h^[69]. Reproduced from Ref.^[69] with permission. Copyright 2016 WILEY-VCH Verlag GmbH & Co. KGaA, Weinheim. (C) Digital image and reaction mechanism of polymerization from VC and AN to P(VN) polymer after heating treatment at 60 °C for 24 h^[116]. Reproduced from Ref.^[116] with permission. Copyright 2019 Royal Society of Chemistry. (D) Illustrations of reaction mechanisms of crosslinking PAMM-based electrolyte and its corresponding application in $LiNi_{0.5}Mn_{1.5}O_4/Li$ cells^[117]. Reproduced from Ref.^[117] with permission. Copyright 2017 American Chemical Society. (E) Photographs and schemes of transformation from liquid electrolyte to quasi-solid electrolyte by thermal crosslinking^[118]. Reproduced from Ref.^[118] with permission. Copyright 2020 Elsevier B.V. (F) Schematic model of the polymerization mechanism of DOL induced by $LiPF_6$ ^[124]. Reproduced from Ref.^[124] with permission. Copyright 2018 The Authors. (G) Photographs of polymerization from VC to PVCA after heating treatment at 60 °C for 24 h with and without LSnPS^[126]. Reproduced from Ref.^[126] with permission. Copyright 2018 American Chemical Society. (H) Cross-sectional morphologies of LAGP-PP separators after different cycles in a LCO/Li cell with respect to 0 and 10 cycles at 0.1C, 380 cycles at 0.5C and 450 cycles at 1C from left to right^[130]. Reproduced from Ref.^[130] with permission. Copyright 2016 Chinese Physical Society and IOP Publishing Ltd. VC: vinylene carbonate.

poly(vinylene carbonate-acrylonitrile) (PVN)-based polymer electrolyte obtained by copolymerizing AN with VC, as shown in Figure 8C^[116]. Density functional theory calculations were employed to prove the electrochemical stability of PVN from the perspective of the lowest HOMO energy level. Benefitting from the $-C \equiv N$ groups in PAN, PVN showed a lower HOMO energy level of -0.3236 eV than that of PVCA. This low HOMO energy level indicated a difficult electron transition, leading to high-voltage tolerance of PVN against $LiNi_{0.5}Mn_{1.5}O_4$.

The solid electrolytes prepared by in-situ crosslinking reactions that induce the bonding and crosslinking of two or more molecules always display 3D network structures, leading to an increase in mechanical properties and thermal stability. Ma *et al.*^[117] proposed a crosslinking network of a poly(acrylic anhydride-2-methyl-acrylic acid-2-oxirane-ethyl ester-methyl methacrylate) (PAMM)-based electrolyte to push the application of solid batteries with high energy density [Figure 8D]. The crosslinking of acrylic anhydride and methyl methacrylate overcomes the low mechanical strength of PMMA. Together, the in-situ polymerization of two monomers inside the battery established intimate contact between the PAMM-based electrolyte and electrodes, resulting in markedly improved cycling performance for the 5 V LiNi_{0.5}Mn_{1.5}O₄/Li cell. Li *et al.*^[118] designed a 3D crosslinking gel network by copolymerizing a poly(ethylene glycol) methyl ether acrylate monomer and crosslinker triethylene glycol diacrylate [Figure 8E]. The polyacrylate served as the main chain and was used to enhance the mechanical strength of the polymer electrolyte, while the ether bond-rich units were crosslinked throughout the framework to promote the ionic transfer. The Li salt in the liquid electrolyte was encapsulated in a polymeric network to endow the membrane with better flexibility. The distinct structure effectively restricted dendrite growth and the pulverization of the Li-metal anode.

The introduction of initiators, such as AIBN, might result in unknown side effects, especially regarding the Li-metal side. To reduce the adverse effects of external additives, researchers have conducted a series of works without extra initiators for polymerization. Zhou *et al.*^[119] made use of PF₅, as a strong Lewis acid produced by the thermal decomposition of LiPF₆, to initiate the in-situ cationic polymerization of cyano resin, leading to the formation of a novel cyanoethyl polyvinyl alcohol electrolyte. Recently, a series of Lewis acids, including LiPF₆, LiDFOB, LiFSI, AlF₃ and Al(OTf)₃, have been investigated to induce the in-situ ring-opening polymerization of ether monomers under room temperature^[101,120-123]. Liu *et al.*^[124] found that PF₅, as a decomposition product of LiPF₆, could combine trace water to form H⁺(PF₅OH)⁻, inducing the fast ring-opening polymerization of DOL monomers [Figure 8F]. Since the polymer network altered the solvation structure of the electrolyte molecules, the electrochemical stability window was enlarged, thereby breaking through the voltage limitation of conventional ether electrolytes. Furthermore, Wu *et al.*^[125] utilized BF₃, which was the decomposition product of LiDFOB from the reaction with alkaline lithium, as an initiator to induce the ring-opening polymerization of 1,3,5-trioxane.

With the continuous development of in-situ polymerization, functional solid electrolytes have also been proposed to meet the higher requirements of high-performance solid batteries with high energy density and safety. Inorganic fillers, including sulfides (*e.g.*, Li₁₀SnP₂S₁₂)^[126] and garnet oxide (Li_{6.25}Ga_{0.25}La₃Zr₂O₁₂)^[127], have been composited with in-situ polymerized polymer electrolytes to improve the ionic conductivity by generating percolation channels and the dendrite suppressing capability by introducing rigid inorganic phases [Figure 8G]. Tan *et al.*^[128] introduced a flame-retardant liquid phosphate into a robust solid polycarbonate matrix by in-situ polymerization. On this basis, an inherently non-flammable electrolyte was in-situ constructed to ensure high battery safety in the case of thermal runaway. Furthermore, both the liquid phosphate and polymer skeleton are electronically insulating, leading to fast Li⁺ transfer across the electrolyte, rather than being reduced to cause dendrite growth. The species of Li salts is also important for constructing stable electrolytes against both the cathode and Li anode. Fan *et al.*^[129] added a dual salt (LiTFSI-LiPF₆) into the crosslinking copolymer of PEGDA and ethoxylated trimethylolpropane triacrylate (ETPTA). The dual-salt system improved the ion conductivity and stability of the SEI film, which was critical for Li dendrite suppression.

Wu *et al.*^[130] proposed the concept of in-situ SEI formation on an ionic conducting separator during charge/discharge cycling. A Li_{1.5}Al_{0.5}Ge_{1.5}(PO₄)₃-coated polypropylene (LAGP-PP) separator filled with liquid electrolyte was adopted as the electrolyte. Figure 8H shows the cross-sectional morphologies of LAGP-PP

separators after different cycles in an LCO/Li cell, where the artificial SEI film was formed on the surface of LAGP particles during cycling. The solidified conversion of the organic liquid to a solid phase not only decreased the liquid content in the battery but also effectively suppressed dendrite growth and ensured long cycle life. However, the stable and homogenous liquid-to-solid conversion induced by such an in-situ electrochemical reaction needs to be considered in large-scale production.

NEW TYPES OF ALL-IN-ONE SOLID BATTERIES

In recent years, with the rapid development of solidification techniques, various new types of solid batteries through upgraded solidification strategies have been proposed to satisfy the requirements of high energy density and safety, including in-situ gradient solidification, all-in-one solidification and so on.

As previously discussed, interfacial issues have their own characteristics with respect to the cathode and anode sides. From the perspective of mechanical performance, the cathode and electrolyte should have an intimate and soft contact for facile ionic transfer, while the electrolyte on the anode side should be mechanically strong for the inhibition of Li dendrite growth. From the perspective of (electro)chemical stability, the electrolyte should be oxidation-resistant when in contact with the cathode and reduction resistant when in contact with the anode. Therefore, it is usually difficult to simultaneously address the interfacial issues on both cathode and anode sides by one-pot solidification.

In this context, many researchers have proposed in-situ gradient solidification with the aim of achieving different interfacial characteristics for the cathode and anode sides. For example, Liu *et al.*^[131] introduced the concept of “functional gradient materials” to solidification in solid batteries. For polymer electrolyte-based solid batteries, Li dendrites can be easily induced and penetrate across the soft electrolyte due to its poor mechanical strength, while composite polymer electrolytes cannot form a uniform structure due to the agglomeration of inorganic fillers, resulting in a lack of continuous domains with high modulus, which also induces dendrites in low-modulus regions. They designed a functional gradient electrolyte consisting of a ceramic-rich layer and a polymer-rich layer with continuous ceramic domains. The compact ceramic-rich layer with a high modulus (6.67 GPa) acted as a physical barrier to prohibit dendrite growth. Furthermore, the soft polymer-rich side with a moderate modulus improved the cathode/electrolyte interface and the conductivity of the electrolyte [Figure 9A]. This gradient structure was greatly compatible with high LFP mass loadings of 11.2 and 15.6 mg cm⁻² [Figure 9B], ensuring the feasibility of the applicable solid battery.

Differing from gradient additives, Wang *et al.*^[132] utilized a gradient Li salt to induce different solidification degrees of organic monomers. LiPF₆ was cast on an Al₂O₃-coated polyethylene (Al₂O₃/PE) separator, followed by infusion with a liquid DOL electrolyte and assembled into a Li-S battery, as shown in Figure 9C. As aforementioned, the decomposition of LiPF₆ triggers the cationic polymerization of DOL. In the Li-S battery, the slow release of LiPF₆ into the DOL electrolyte induced gradient solidification at the cathode/electrolyte interface, i.e., a polymer-based gel electrolyte was generated on the cathode surface while a liquid electrolyte was kept inside the cathode [Figure 9D]. The distinct electrolyte configuration contributed to the moderate dissolution of discharge products inside the cathode while preventing the shuttle of soluble intermediates away from the cathode.

Xiao *et al.*^[67] proposed a “melt infiltration” technique by using an anti-perovskite solid electrolyte (Li_{1.9}OHCl_{0.9}) with a low melting point of ~300 °C. Limited by the melting of Li metal above 180 °C, the Li_{1.9}OHCl_{0.9} solid electrolyte suffered from the “heating-cooling” process by a combination of a LiNi_{0.33}Mn_{0.33}Co_{0.33}O₂ cathode and Li₄Ti₅O₁₂ or graphite anodes [Figure 9E]. The electrolyte in a molten state was fully infiltrated into thermally stable electrodes at moderate temperature (~300 °C), after which the melt seamlessly

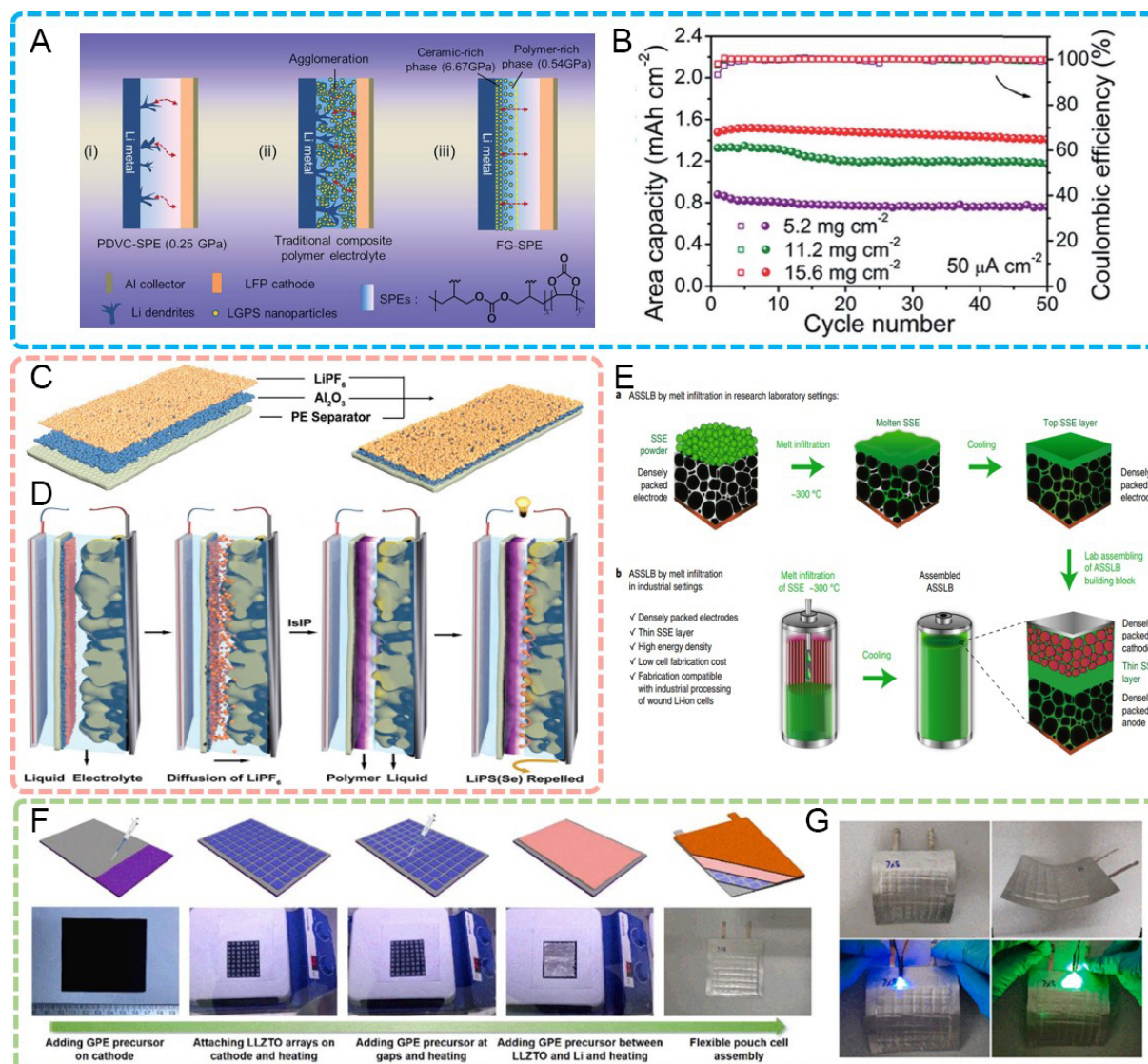


Figure 9. (A) Schematic working principle of solid batteries with polymer, composite and gradient electrolytes with an asymmetric distribution of polymers and ceramic fillers^[131]. Reproduced from Ref.^[131] with permission. Copyright 2019 Royal Society of Chemistry. (B) Cycling performance of LFP battery at high mass loadings of 11.2 and 15.6 mg cm⁻² with gradient electrolytes^[131]. Reproduced from Ref.^[131] with permission. Copyright 2019 Royal Society of Chemistry. (C) Structure of LiPF₆-modified Al₂O₃/PE separator^[132]. Reproduced from Ref.^[132] with permission. Copyright 2020 WILEY-VCH Verlag GmbH & Co. KGaA, Weinheim. (D) Schematic formation process of in-situ interfacial polymerization of DOL-based liquid electrolyte realized by LiPF₆/Al₂O₃/PE separator^[132]. Reproduced from Ref.^[132] with permission. Copyright 2020 WILEY-VCH Verlag GmbH & Co. KGaA, Weinheim. (E) Illustration of melt infiltration in research laboratory and industrial settings^[67]. Reproduced from Ref.^[67] with permission. Copyright 2021 Springer Nature. (F) Preparation of flexible and large-scale solid garnet batteries by introducing in-situ solidified gel polymer electrolytes^[70]. Reproduced from Ref.^[70] with permission. Copyright 2021 Elsevier Ltd. (G) Solid garnet batteries can be bent and used to power blue/green LEDs^[70]. LFP: LiFePO₄. Reproduced from Ref.^[70] with permission. Copyright 2021 Elsevier Ltd.

solidified into a solid state during cooling for low-resistance interfaces and minimum cell volume. Furthermore, the all-in-one cell manufacturing process is highly compatible with current commercial technology, which markedly reduces the barrier for industrial adoption.

With the exception of cathode/electrolyte and Li/electrolyte interfaces, in-situ solidification can also take place between small electrolyte blocks to enlarge the area of the solid electrolyte. Generally, the well-known

garnet-type LLZO, as an inorganic ceramic, shows low ductility, leading to its easy fracture when microcracks are produced in its interior under an external force. Therefore, the realization of the large-scale production of LLZO solid electrolytes appears impossible, let alone the flexibility. The in-situ thermal polymerization of ETPTA monomers with LiPF_6 took place not only at the electrode/LLZO interface but also in between the small LLZO blocks^[70] [Figure 9F]. For dual-interface optimization, this work also achieved the coexistence of flexibility and large-scale fabrication for solid garnet batteries by employing solidified electrolytes as adhesives [Figure 9G].

CONCLUSIONS AND OUTLOOK

Advanced SSLBs that couple solid electrolytes with Li anodes present significant potential for the realization of high safety and energy density. However, the practical energy density of solid batteries is limited by the cathode mass loading, electrolyte thickness and anode stability. Furthermore, the significant interfacial challenges associated with the poor physical/(electro)chemical contacts between the electrodes and electrolytes severely impact the cycling performance.

Fortunately, the rational use of solidification that converts liquid precursors into solid phases inside the batteries enables the construction of all-in-one battery configurations with low-resistance, compatible and stable electrode/electrolyte interfaces, leading to the achievement of high energy density and cycling performance. In this review, we have organized the critical requirements for high-energy-density SSLBs from the aspects of cathodes, electrolyte layers, anodes and multiscale interfaces. We have divided the current solidification strategies into the four categories of evaporation, heating-cooling, polymerization and electrochemistry for an easy understanding of the concept, design and mechanisms of different solidifications. Considering the characteristics of different battery components, we have summarized the recent progress of solidifications in applications in the fields of cathodes, anodes and electrolyte layers. In addition, the upgraded solidification strategies toward new types of all-in-one solid batteries have been further reviewed. Solidification gives rise to the reinforcement of interfacial contact and the thickness optimization of each layer, thereby presenting significant potential in breaking the energy density and cycle life bottlenecks for SSLBs.

The application of solidification demonstrates promising prospects in driving the implementation of high-performance solid batteries. However, further endeavors are needed toward mechanism investigations and practical large-scale industrial applications, particularly regarding the challenges listed below:

(1) Characterization and regulation of residual liquid content. Generally, the liquid precursor cannot completely transform into a solid phase by solidification. In order to maintain the solid state of SSLBs to an extreme, the content of residual liquid should be controlled below 5 wt.% of the total solid battery. In addition, it is also difficult to accurately characterize the residual liquid content inside the battery. The mass difference of disassembled batteries before and after the vacuum evaporation treatment has been reported to be the residual liquid content. This measurement is an estimate as the partial residual liquid might be anchored inside the solid matrix, which cannot be completely dried up. Other measurements, like thermogravimetry, have been carried out, yet the result is usually difficult to distinguish, especially when the liquid and solid components have close volatilization or decomposition temperatures. Thus, advanced measurements to accurately obtain the residual liquid content remain challenging.

(2) Research of interfacial chemistry. The formation mechanism of CEI/SEI layers at the solid-solid or solid-liquid interface needs to be clarified. This is also significant for the understanding of interfacial chemistry, as well as preventing undesirable reactions, to acquire a controllable and stable interlayer during repeated

cycling.

(3) Compatibility with both high-voltage cathodes and Li anodes. The realization of high energy density needs the cooperation of high-voltage cathodes and Li-metal anodes. However, the solidification of a liquid precursor with a single component generally cannot satisfy the stability against both the cathode and anode. Therefore, the development of new functional electrolytes together with the solidification strategies is important.

(4) Constructing the seamless interface during the whole battery operation. The solidification guarantees the perfect interfacial contact in the initial cycles. However, the volume changes for the electrode materials during repeated cycling will induce phase separation, leading to gradual contact loss. Controlling the solidification process to ensure a seamless interface during the whole battery lifetime is challenging.

(5) New types of functional solidification. Gradient, asymmetric, ultrathin or multilayered functional solidification should be developed for the further improvement of energy density and interfacial stability. In addition, since the use of a liquid may lead to a decrease in battery safety, some flame-retardant polymer electrolytes or additives should be combined with the solidification to achieve high-safety solid batteries.

(6) Actual realization of high energy density. According to the calculation of energy density, the cathode should have a high mass loading and a large thickness, while the electrolyte and Li metal should be thin and lightweight. Although solidification enables a high mass loading to some extent, the continuous increase of cathode mass loading up to industrial grade inevitably causes performance attenuation. Thus, the actual realization of high practical energy density remains difficult.

(7) Compatibility with current industrial technology. The boost of the practical application of solid batteries should be compatible with the current industrial technology considering cost issues. Although solidification is similar to the technique for liquid batteries, some distinct post-treatments, like heating, cooling or irradiating, should be considered for the industrialization of applicable solid batteries.

In spite of these challenges, solidification is considered as a promising strategy for the breakthrough of solid batteries in terms of energy density and interface improvement. More effort should be devoted to both the design and mechanism exploration of various solidification strategies toward practical applications. As the most compatible technology with the current industrial technology, we believe that the solidification will be extensively adopted in next-generation high-performance SSLBs in the near future.

DECLARATIONS

Authors' contributions

Preparing the manuscript draft: Bi Z

Writing-review and editing, funding acquisition, supervision: Guo X

Availability of data and materials

Not applicable.

Financial support and sponsorship

This work was supported by the National Natural Science Foundation of China (Grant No. 22005163, and U1932205), the Key R&D Program of Shandong Province (Grant No. 2021CXGC010401), the "Taishan Scholars Program" (Grant No. ts201712035), and the Project of Qingdao Leading Talents in

Entrepreneurship and Innovation.

Conflicts of interest

All authors declared that there are no conflicts of interest.

Ethical approval and consent to participate

Not applicable.

Consent for publication

Not applicable.

Copyright

© The Author(s) 2022.

REFERENCES

1. Chen R, Li Q, Yu X, Chen L, Li H. Approaching practically accessible solid-state batteries: stability issues related to solid electrolytes and interfaces. *Chem Rev* 2020;120:6820-77. DOI PubMed
2. Zu C, Yu H, Li H. Enabling the thermal stability of solid electrolyte interphase in Li-ion battery. *InfoMat* 2021;3:648-61. DOI
3. Yang C, Zhang L, Liu B, et al. Continuous plating/stripping behavior of solid-state lithium metal anode in a 3D ion-conductive framework. *Proc Natl Acad Sci U S A* 2018;115:3770-5. DOI PubMed PMC
4. Jia M, Zhao N, Huo H, Guo X. Comprehensive investigation into garnet electrolytes toward application-oriented solid lithium batteries. *Electrochem Energ Rev* 2020;3:656-89. DOI
5. Zhao N, Khokhar W, Bi Z, et al. Solid garnet batteries. *Joule* 2019;3:1190-9. DOI
6. Wang L, Zhang X, Wang T, et al. Ameliorating the interfacial problems of cathode and solid-state electrolytes by interface modification of functional polymers. *Adv Energy Mater* 2018;8:1801528. DOI
7. Hatzell KB, Chen XC, Cobb CL, et al. Challenges in lithium metal anodes for solid-state batteries. *ACS Energy Lett* 2020;5:922-34. DOI
8. Duan H, Fan M, Chen WP, et al. Extended electrochemical window of solid electrolytes via heterogeneous multilayered structure for high-voltage lithium metal batteries. *Adv Mater* 2019;31:e1807789. DOI PubMed
9. Yuan S, Kong T, Zhang Y, et al. Advanced electrolyte design for high-energy-density Li-metal batteries under practical conditions. *Angew Chem Int Ed Engl* 2021;60:25624-38. DOI PubMed
10. Duan H, Chen WP, Fan M, et al. Building an air stable and lithium deposition regulable garnet interface from moderate-temperature conversion chemistry. *Angew Chem Int Ed Engl* 2020;59:12069-75. DOI PubMed
11. Deng T, Ji X, Zhao Y, et al. Tuning the anode-electrolyte interface chemistry for garnet-based solid-state Li metal batteries. *Adv Mater* 2020;32:e2000030. DOI PubMed
12. Fu X, Wang T, Shen W, et al. A high-performance carbonate-free lithium|garnet interface enabled by a trace amount of sodium. *Adv Mater* 2020;32:e2000575. DOI PubMed
13. Liang JY, Zeng XX, Zhang XD, et al. Mitigating interfacial potential drop of cathode-solid electrolyte via ionic conductor layer to enhance interface dynamics for solid batteries. *J Am Chem Soc* 2018;140:6767-70. DOI PubMed
14. Cao D, Zhao Y, Sun X, et al. Processing strategies to improve cell-level energy density of metal sulfide electrolyte-based all-solid-state li metal batteries and beyond. *ACS Energy Lett* 2020;5:3468-89. DOI
15. Bi Z, Zhao N, Ma L, et al. Surface coating of LiMn₂O₄ cathodes with garnet electrolytes for improving cycling stability of solid lithium batteries. *J Mater Chem A* 2020;8:4252-6. DOI
16. Yoon K, Lee S, Oh K, Kang K. Challenges and strategies towards practically feasible solid-state lithium metal batteries. *Adv Mater* 2022;34:e2104666. DOI PubMed
17. Liu J, Yuan H, Liu H, et al. Unlocking the failure mechanism of solid state lithium metal batteries. *Advanced Energy Materials* 2022;12:2100748. DOI
18. Zhao C, Zhao B, Yan C, et al. Liquid phase therapy to solid electrolyte-electrode interface in solid-state Li metal batteries: a review. *Energy Storage Materials* 2020;24:75-84. DOI
19. Bi Z, Zhao N, Ma L, et al. Interface engineering on cathode side for solid garnet batteries. *Chemical Engineering Journal* 2020;387:124089. DOI
20. Wu C, Lou J, Zhang J, et al. Current status and future directions of all-solid-state batteries with lithium metal anodes, sulfide electrolytes, and layered transition metal oxide cathodes. *Nano Energy* 2021;87:106081. DOI
21. Cao C, Liang F, Zhang W, et al. Commercialization-driven electrodes design for lithium batteries: basic guidance, opportunities, and perspectives. *Small* 2021;17:e2102233. DOI PubMed
22. Liu Q, Geng Z, Han C, et al. Challenges and perspectives of garnet solid electrolytes for all solid-state lithium batteries. *Journal of*

- Power Sources* 2018;389:120-34. DOI
23. Cui G. Reasonable design of high-energy-density solid-state lithium-metal batteries. *Matter* 2020;2:805-15. DOI
 24. Zhu J, Xiang Y, Zhao J, et al. Insights into the local structure, microstructure and ionic conductivity of silicon doped nasicon-type solid electrolyte $\text{Li}_{1.3}\text{Al}_{0.3}\text{Ti}_{1.7}\text{P}_3\text{O}_{12}$. *Energy Storage Materials* 2022;44:190-6. DOI
 25. Liang F, Sun Y, Yuan Y, Huang J, Hou M, Lu J. Designing inorganic electrolytes for solid-state Li-ion batteries: a perspective of LGPS and garnet. *Materials Today* 2021;50:418-41. DOI
 26. Wang C, Ping W, Bai Q, et al. A general method to synthesize and sinter bulk ceramics in seconds. *Science* 2020;368:521-6. DOI PubMed
 27. Xu Q, Tsai C, Song D, et al. Insights into the reactive sintering and separated specific grain/grain boundary conductivities of $\text{Li}_{1.3}\text{Al}_{0.3}\text{Ti}_{1.7}(\text{PO}_4)_3$. *Journal of Power Sources* 2021;492:229631. DOI
 28. Wu J, Yuan L, Zhang W, Li Z, Xie X, Huang Y. Reducing the thickness of solid-state electrolyte membranes for high-energy lithium batteries. *Energy Environ Sci* 2021;14:12-36. DOI
 29. Yang X, Adair KR, Gao X, Sun X. Recent advances and perspectives on thin electrolytes for high-energy-density solid-state lithium batteries. *Energy Environ Sci* 2021;14:643-71. DOI
 30. Mu S, Bi Z, Gao S, Guo X. Combination of organic and inorganic electrolytes for composite membranes toward applicable solid lithium batteries. *Chem Res Chin Univ* 2021;37:246-53. DOI
 31. Chen L, Li Y, Li S, Fan L, Nan C, Goodenough JB. PEO/garnet composite electrolytes for solid-state lithium batteries: from “ceramic-in-polymer” to “polymer-in-ceramic”. *Nano Energy* 2018;46:176-84. DOI
 32. Zhang X, Liu T, Zhang S, et al. Synergistic coupling between $\text{Li}_{6.75}\text{La}_3\text{Zr}_{1.75}\text{Ta}_{0.25}\text{O}_{12}$ and poly(vinylidene fluoride) induces high ionic conductivity, mechanical strength, and thermal stability of solid composite electrolytes. *J Am Chem Soc* 2017;139:13779-85. DOI PubMed
 33. Jia M, Zhao N, Bi Z, et al. Polydopamine-coated garnet particles homogeneously distributed in poly(propylene carbonate) for the conductive and stable membrane electrolytes of solid lithium batteries. *ACS Appl Mater Interfaces* 2020;12:46162-9. DOI PubMed
 34. Jia M, Bi Z, Shi C, Zhao N, Guo X. Polydopamine coated lithium lanthanum titanate in bilayer membrane electrolytes for solid lithium batteries. *ACS Appl Mater Interfaces* 2020;12:46231-8. DOI PubMed
 35. Liu L, Qi X, Yin S, et al. In situ formation of a stable interface in solid-state batteries. *ACS Energy Lett* 2019;4:1650-7. DOI
 36. Cho SM, Shim J, Cho SH, et al. Quasi-solid-state rechargeable Li-O₂ batteries with high safety and long cycle life at room temperature. *ACS Appl Mater Interfaces* 2018;10:15634-41. DOI PubMed
 37. Hua S, Jing M, Han C, et al. A novel titania nanorods-filled composite solid electrolyte with improved room temperature performance for solid-state Li-ion battery. *Int J Energy Res* 2019. DOI
 38. Chen H, Jing M, Han C, et al. A novel organic/inorganic composite solid electrolyte with functionalized layers for improved room-temperature rate performance of solid-state lithium battery. *Int J Energy Res* 2019;43:5912-21. DOI
 39. Zhang J, Zang X, Wen H, et al. High-voltage and free-standing poly(propylene carbonate)/ $\text{Li}_{6.75}\text{La}_3\text{Zr}_{1.75}\text{Ta}_{0.25}\text{O}_{12}$ composite solid electrolyte for wide temperature range and flexible solid lithium ion battery. *J Mater Chem A* 2017;5:4940-8. DOI
 40. Bonizzoni S, Ferrara C, Berbenni V, Anselmi-Tamburini U, Mustarelli P, Tealdi C. NASICON-type polymer-in-ceramic composite electrolytes for lithium batteries. *Phys Chem Chem Phys* 2019;21:6142-9. DOI PubMed
 41. Liu W, Liu N, Sun J, et al. Ionic conductivity enhancement of polymer electrolytes with ceramic nanowire fillers. *Nano Lett* 2015;15:2740-5. DOI PubMed
 42. Zhang J, Zhao N, Zhang M, et al. Flexible and ion-conducting membrane electrolytes for solid-state lithium batteries: dispersion of garnet nanoparticles in insulating polyethylene oxide. *Nano Energy* 2016;28:447-54. DOI
 43. Chen H, Yang Y, Boyle DT, et al. Free-standing ultrathin lithium metal-graphene oxide host foils with controllable thickness for lithium batteries. *Nat Energy* 2021;6:790-8. DOI
 44. Ye Y, Zhao Y, Zhao T, et al. An antipulverization and high-continuity lithium metal anode for high-energy lithium batteries. *Adv Mater* 2021:e2105029. DOI PubMed
 45. Sun Y, Li F, Hou P. Research progress on the interfaces of solid-state lithium metal batteries. *J Mater Chem A* 2021;9:9481-505. DOI
 46. Li C, Zhang X, Zhu Y, et al. Modulating the lithiophilicity at electrode/electrolyte interface for high-energy Li-metal batteries. *EM* 2021. DOI
 47. Ruan Y, Lu Y, Huang X, et al. Acid induced conversion towards a robust and lithiophilic interface for Li-Li₇La₃Zr₂O₁₂ solid-state batteries. *J Mater Chem A* 2019;7:14565-74. DOI
 48. Ruan Y, Lu Y, Li Y, et al. A 3D Cross-linking lithiophilic and electronically insulating interfacial engineering for garnet-type solid-state lithium batteries. *Adv Funct Mater* 2021;31:2007815. DOI
 49. Pan X, Sun H, Wang Z, et al. High Voltage stable polyoxalate catholyte with cathode coating for all-solid-state Li-metal/nmc622 batteries. *Adv Energy Mater* 2020;10:2002416. DOI
 50. Zhu Y, He X, Mo Y. First principles study on electrochemical and chemical stability of solid electrolyte-electrode interfaces in all-solid-state Li-ion batteries. *J Mater Chem A* 2016;4:3253-66. DOI
 51. Nolan AM, Wachsmann ED, Mo Y. Computation-guided discovery of coating materials to stabilize the interface between lithium garnet solid electrolyte and high-energy cathodes for all-solid-state lithium batteries. *Energy Storage Materials* 2021;41:571-80. DOI
 52. Stegmaier S, Schierholz R, Povstugar I, et al. Nano-scale complexions facilitate Li dendrite-free operation in LATP solid-state

- electrolyte. *Adv Energy Mater* 2021;11:2100707. DOI
53. Mu S, Huang W, Sun W, et al. Heterogeneous electrolyte membranes enabling double-side stable interfaces for solid lithium batteries. *Journal of Energy Chemistry* 2021;60:162-8. DOI
 54. Jiang T, He P, Liang Y, Fan L. All-dry synthesis of self-supporting thin $\text{Li}_{10}\text{GeP}_2\text{S}_{12}$ membrane and interface engineering for solid state lithium metal batteries. *Chemical Engineering Journal* 2021;421:129965. DOI
 55. Wang C, Yu R, Duan H, et al. Solvent-free approach for interweaving freestanding and ultrathin inorganic solid electrolyte membranes. *ACS Energy Lett* 2022;7:410-6. DOI
 56. Han F, Westover AS, Yue J, et al. High electronic conductivity as the origin of lithium dendrite formation within solid electrolytes. *Nat Energy* 2019;4:187-96. DOI
 57. Han F, Yue J, Chen C, et al. Interphase engineering enabled all-ceramic lithium battery. *Joule* 2018;2:497-508. DOI
 58. Wang C, Sun Q, Liu Y, et al. Boosting the performance of lithium batteries with solid-liquid hybrid electrolytes: interfacial properties and effects of liquid electrolytes. *Nano Energy* 2018;48:35-43. DOI
 59. Liu B, Gong Y, Fu K, et al. Garnet solid electrolyte protected li-metal batteries. *ACS Appl Mater Interfaces* 2017;9:18809-15. DOI PubMed
 60. Randau S, Weber DA, Kötz O, et al. Benchmarking the performance of all-solid-state lithium batteries. *Nat Energy* 2020;5:259-70. DOI
 61. Zhou W, Wang Z, Pu Y, et al. Double-layer polymer electrolyte for high-voltage all-solid-state rechargeable batteries. *Adv Mater* 2019;31:e1805574. DOI PubMed
 62. Kim JH, Go K, Lee KJ, Kim HS. Improved performance of all-solid-state lithium metal batteries via physical and chemical interfacial control. *Adv Sci (Weinh)* 2022;9:e2103433. DOI PubMed PMC
 63. Liu W, Yi C, Li L, et al. Designing polymer-in-salt electrolyte and fully infiltrated 3d electrode for integrated solid-state lithium batteries. *Angew Chem Int Ed Engl* 2021;60:12931-40. DOI PubMed
 64. Bi Z, Mu S, Zhao N, Sun W, Huang W, Guo X. Cathode supported solid lithium batteries enabling high energy density and stable cyclability. *Energy Storage Materials* 2021;35:512-9. DOI
 65. Alarco PJ, Abu-Lebdeh Y, Abouimrane A, Armand M. The plastic-crystalline phase of succinonitrile as a universal matrix for solid-state ionic conductors. *Nat Mater* 2004;3:476-81. DOI PubMed
 66. Xin C, Wen K, Xue C, et al. Composite cathodes with succinonitrile-based ionic conductors for long-cycle-life solid-state lithium metal batteries. *Batteries & Supercaps* 2022;5:e202100162. DOI
 67. Xiao Y, Turcheniuk K, Narla A, et al. Electrolyte melt infiltration for scalable manufacturing of inorganic all-solid-state lithium-ion batteries. *Nat Mater* 2021;20:984-90. DOI PubMed
 68. Kerman K, Luntz A, Viswanathan V, Chiang Y, Chen Z. Review - practical challenges hindering the development of solid state li ion batteries. *J Electrochem Soc* 2017;164:A1731-44. DOI
 69. Chai J, Liu Z, Ma J, et al. In situ generation of poly (vinylene carbonate) based solid electrolyte with interfacial stability for LiCoO_2 Lithium Batteries. *Adv Sci (Weinh)* 2017;4:1600377. DOI PubMed PMC
 70. Bi Z, Huang W, Mu S, Sun W, Zhao N, Guo X. Dual-interface reinforced flexible solid garnet batteries enabled by in-situ solidified gel polymer electrolytes. *Nano Energy* 2021;90:106498. DOI
 71. Choi K, Cho S, Kim S, Kwon YH, Kim JY, Lee S. Thin, deformable, and safety-reinforced plastic crystal polymer electrolytes for high-performance flexible lithium-ion batteries. *Adv Funct Mater* 2014;24:44-52. DOI
 72. Lv Z, Zhou Q, Zhang S, et al. Cyano-reinforced in-situ polymer electrolyte enabling long-life cycling for high-voltage lithium metal batteries. *Energy Storage Materials* 2021;37:215-23. DOI
 73. Liu X, Ding G, Zhou X, et al. An interpenetrating network poly(diethylene glycol carbonate)-based polymer electrolyte for solid state lithium batteries. *J Mater Chem A* 2017;5:11124-30. DOI
 74. Cho YG, Hwang C, Cheong DS, Kim YS, Song HK. Gel/solid polymer electrolytes characterized by in situ gelation or polymerization for electrochemical energy systems. *Adv Mater* 2019;31:e1804909. DOI PubMed
 75. Zhang J, Yang J, Wu H, et al. Research progress of in situ generated polymer electrolyte for rechargeable batteries. *Acta Polymerica Sinica* 2019;50:890-914. DOI
 76. Nolan AM, Liu Y, Mo Y. Solid-state chemistries stable with high-energy cathodes for lithium-ion batteries. *ACS Energy Lett* 2019;4:2444-51. DOI
 77. Goodenough JB, Kim Y. Challenges for rechargeable Li batteries. *Chem Mater* 2010;22:587-603. DOI PubMed
 78. Zhou Q, Ma J, Dong S, Li X, Cui G. Intermolecular chemistry in solid polymer electrolytes for high-energy-density lithium batteries. *Adv Mater* 2019;31:e1902029. DOI PubMed
 79. Hou J, Yang M, Wang D, Zhang J. Fundamentals and challenges of lithium ion batteries at temperatures between -40 and 60 °C. *Adv Energy Mater* 2020;10:1904152. DOI
 80. Gao Y, Wang D, Li YC, Yu Z, Mallouk TE, Wang D. Salt-based organic-inorganic nanocomposites: towards a stable lithium metal/ $\text{Li}_{10}\text{GeP}_2\text{S}_{12}$ solid electrolyte interface. *Angew Chem Int Ed Engl* 2018;57:13608-12. DOI PubMed
 81. Umeshbabu E, Zheng B, Zhu J, Wang H, Li Y, Yang Y. Stable cycling lithium-sulfur solid batteries with enhanced $\text{Li}/\text{Li}_{10}\text{GeP}_2\text{S}_{12}$ solid electrolyte interface stability. *ACS Appl Mater Interfaces* 2019;11:18436-47. DOI PubMed
 82. Caradant L, Verdier N, Foran G, et al. Extrusion of polymer blend electrolytes for solid-state lithium batteries: a study of polar functional groups. *ACS Appl Polym Mater* 2021;3:6694-704. DOI

83. Li L, Deng Y, Duan H, Qian Y, Chen G. LiF and LiNO₃ as synergistic additives for PEO-PVDF/LLZTO-based composite electrolyte towards high-voltage lithium batteries with dual-interfaces stability. *Journal of Energy Chemistry* 2022;65:319-28. DOI
84. Qiu J, Liu X, Chen R, et al. Enabling stable cycling of 4.2 V high-voltage all-solid-state batteries with PEO-based solid electrolyte. *Adv Funct Mater* 2020;30:1909392. DOI
85. Liang J, Hwang S, Li S, et al. Stabilizing and understanding the interface between nickel-rich cathode and PEO-based electrolyte by lithium niobium oxide coating for high-performance all-solid-state batteries. *Nano Energy* 2020;78:105107. DOI
86. Chen X, He W, Ding L, Wang S, Wang H. Enhancing interfacial contact in all solid state batteries with a cathode-supported solid electrolyte membrane framework. *Energy Environ Sci* 2019;12:938-44. DOI
87. Lin Y, Wu M, Sun J, Zhang L, Jian Q, Zhao T. A high-capacity, long-cycling all-solid-state lithium battery enabled by integrated cathode/ultrathin solid electrolyte. *Adv Energy Mater* 2021;11:2101612. DOI
88. Lin Y, Liu K, Wu M, Zhao C, Zhao T. Enabling solid-state Li metal batteries by in situ forming ionogel interlayers. *ACS Appl Energy Mater* 2020;3:5712-21. DOI
89. Wei Z, Chen S, Wang J, et al. Superior lithium ion conduction of polymer electrolyte with comb-like structure via solvent-free copolymerization for bipolar all-solid-state lithium battery. *J Mater Chem A* 2018;6:13438-47. DOI
90. Wei Z, Chen S, Wang J, et al. A large-size, bipolar-stacked and high-safety solid-state lithium battery with integrated electrolyte and cathode. *Journal of Power Sources* 2018;394:57-66. DOI
91. Nie K, Wang X, Qiu J, et al. Increasing poly(ethylene oxide) stability to 4.5 v by surface coating of the cathode. *ACS Energy Lett* 2020;5:826-32. DOI
92. Lu J, Zhou J, Chen R, et al. 4.2 V poly(ethylene oxide)-based all-solid-state lithium batteries with superior cycle and safety performance. *Energy Storage Materials* 2020;32:191-8. DOI
93. Ma J, Liu Z, Chen B, et al. A strategy to make high voltage LiCoO₂ compatible with polyethylene oxide electrolyte in all-solid-state lithium ion batteries. *J Electrochem Soc* 2017;164:A3454-61. DOI
94. Kim DH, Oh DY, Park KH, et al. Infiltration of solution-processable solid electrolytes into conventional Li-ion-battery electrodes for all-solid-state Li-ion batteries. *Nano Lett* 2017;17:3013-20. DOI PubMed
95. Xiao Y, Xu R, Xu L, Ding J, Huang J. Recent advances on anion-derived SEI for fast-charging and stable lithium batteries. *Energy Mater* 2021;1:100013. DOI
96. Zhang Q, Pan K, Jia M, et al. Ionic liquid additive stabilized cathode/electrolyte interface in LiCoO₂ based solid-state lithium metal batteries. *Electrochimica Acta* 2021;368:137593. DOI
97. Feng W, Yang P, Dong X, Xia Y. A Low temperature soldered all ceramic lithium battery. *ACS Appl Mater Interfaces* 2022;14:1149-56. DOI PubMed
98. Chen Y, Huo F, Chen S, Cai W, Zhang S. In-built quasi-solid-state poly-ether electrolytes enabling stable cycling of high-voltage and wide-temperature Li metal batteries. *Adv Funct Mater* 2021;31:2102347. DOI
99. Qiu J, Yang L, Sun G, Yu X, Li H, Chen L. A stabilized PEO-based solid electrolyte via a facile interfacial engineering method for a high voltage solid-state lithium metal battery. *Chem Commun (Camb)* 2020;56:5633-6. DOI PubMed
100. Huang W, Bi Z, Zhao N, Sun Q, Guo X. Chemical interface engineering of solid garnet batteries for long-life and high-rate performance. *Chemical Engineering Journal* 2021;424:130423. DOI
101. Zhao CZ, Zhao Q, Liu X, et al. Rechargeable lithium metal batteries with an in-built solid-state polymer electrolyte and a high voltage/loading Ni-rich layered cathode. *Adv Mater* 2020;32:e1905629. DOI PubMed
102. Zhang S, Zeng Z, Zhai W, Hou G, Chen L, Ci L. Bifunctional in situ polymerized interface for stable LAGP-based lithium metal batteries. *Adv Materials Inter* 2021;8:2100072. DOI
103. Zeng XX, Yin YX, Li NW, Du WC, Guo YG, Wan LJ. Reshaping lithium plating/stripping behavior via bifunctional polymer electrolyte for room-temperature solid Li metal batteries. *J Am Chem Soc* 2016;138:15825-8. DOI PubMed
104. Duan H, Yin YX, Shi Y, et al. Dendrite-free Li-metal battery enabled by a thin asymmetric solid electrolyte with engineered layers. *J Am Chem Soc* 2018;140:82-5. DOI PubMed
105. Chai J, Chen B, Xian F, et al. Dendrite-free lithium deposition via flexible-rigid coupling composite network for LiNi_{0.5}Mn_{1.5}O₄ /Li metal batteries. *Small* 2018;14:e1802244. DOI PubMed
106. Zhang X, Chen X, Hou L, et al. Regulating anions in the solvation sheath of lithium ions for stable lithium metal batteries. *ACS Energy Lett* 2019;4:411-6. DOI
107. Zheng B, Zhu J, Wang H, et al. Stabilizing Li₁₀SnP₂S₁₂/Li interface via an in situ formed solid electrolyte interphase layer. *ACS Appl Mater Interfaces* 2018;10:25473-82. DOI PubMed
108. Tong Z, Wang SB, Jena A, et al. Matchmaker of marriage between a Li metal anode and NASICON-structured solid-state electrolyte: plastic crystal electrolyte and three-dimensional host structure. *ACS Appl Mater Interfaces* 2020;12:44754-61. DOI PubMed
109. Zhu X, Chang Z, Yang H, He P, Zhou H. Highly safe and stable lithium-metal batteries based on a quasi-solid-state electrolyte. *J Mater Chem A* 2022;10:651-63. DOI
110. Cao W, Yang Y, Deng J, Li Y, Cui C, Zhang T. Localization of electrons within interlayer stabilizes NASICON-type solid-state electrolyte. *Materials Today Energy* 2021;22:100875. DOI
111. Liu Q, Yu Q, Li S, et al. Safe LAGP-based all solid-state Li metal batteries with plastic super-conductive interlayer enabled by in-situ solidification. *Energy Storage Materials* 2020;25:613-20. DOI
112. Wang C, Adair KR, Liang J, et al. Solid-state plastic crystal electrolytes: effective protection interlayers for sulfide-based all-solid-

- state lithium metal batteries. *Adv Funct Mater* 2019;29:1900392. DOI
113. Ma C, Cui W, Liu X, Ding Y, Wang Y. In situ preparation of gel polymer electrolyte for lithium batteries: progress and perspectives. *InfoMat* 2022;4:e1223. DOI
114. Castillo J, Qiao L, Santiago A, et al. Perspective of polymer-based solid-state Li-S batteries. *Energy Mater* 2022;2:200003. DOI
115. Lin Z, Guo X, Wang Z, et al. A wide-temperature superior ionic conductive polymer electrolyte for lithium metal battery. *Nano Energy* 2020;73:104786. DOI
116. Wang P, Chai J, Zhang Z, et al. An intricately designed poly(vinylene carbonate-acrylonitrile) copolymer electrolyte enables 5 V lithium batteries. *J Mater Chem A* 2019;7:5295-304. DOI
117. Ma Y, Ma J, Chai J, et al. Two players make a formidable combination: in situ generated poly(acrylic anhydride-2-methyl-acrylic acid-2-oxirane-ethyl ester-methyl methacrylate) cross-linking gel polymer electrolyte toward 5 V high-voltage batteries. *ACS Appl Mater Interfaces* 2017;9:41462-72. DOI PubMed
118. Li Z, Zhou X, Guo X. High-performance lithium metal batteries with ultraconformal interfacial contacts of quasi-solid electrolyte to electrodes. *Energy Storage Materials* 2020;29:149-55. DOI
119. Zhou D, He Y, Cai Q, et al. Investigation of cyano resin-based gel polymer electrolyte: in situ gelation mechanism and electrode-electrolyte interfacial fabrication in lithium-ion battery. *J Mater Chem A* 2014;2:20059-66. DOI
120. Sun M, Zeng Z, Peng L, et al. Ultrathin polymer electrolyte film prepared by in situ polymerization for lithium metal batteries. *Materials Today Energy* 2021;21:100785. DOI
121. Liu Q, Cai B, Li S, et al. Long-cycling and safe lithium metal batteries enabled by the synergetic strategy of ex situ anodic pretreatment and an in-built gel polymer electrolyte. *J Mater Chem A* 2020;8:7197-204. DOI
122. Zhao Q, Liu X, Stalin S, Khan K, Archer LA. Solid-state polymer electrolytes with in-built fast interfacial transport for secondary lithium batteries. *Nat Energy* 2019;4:365-73. DOI
123. Cheng H, Zhu J, Jin H, et al. In situ initiator-free gelation of highly concentrated lithium bis(fluorosulfonyl)imide-1,3-dioxolane solid polymer electrolyte for high performance lithium-metal batteries. *Materials Today Energy* 2021;20:100623. DOI
124. Liu FQ, Wang WP, Yin YX, et al. Upgrading traditional liquid electrolyte via in situ gelation for future lithium metal batteries. *Sci Adv* 2018;4:eaat5383. DOI PubMed PMC
125. Wu H, Tang B, Du X, et al. LiDFOB initiated in situ polymerization of novel eutectic solution enables room-temperature solid lithium metal batteries. *Adv Sci (Weinh)* 2020;7:2003370. DOI PubMed PMC
126. Ju J, Wang Y, Chen B, et al. Integrated interface strategy toward room temperature solid-state lithium batteries. *ACS Appl Mater Interfaces* 2018;10:13588-97. DOI PubMed
127. Li Z, Xie H, Zhang X, Guo X. In situ thermally polymerized solid composite electrolytes with a broad electrochemical window for all-solid-state lithium metal batteries. *J Mater Chem A* 2020;8:3892-900. DOI
128. Tan S, Yue J, Tian Y, et al. In-situ encapsulating flame-retardant phosphate into robust polymer matrix for safe and stable quasi-solid-state lithium metal batteries. *Energy Storage Materials* 2021;39:186-93. DOI
129. Fan W, Li NW, Zhang X, et al. A dual-salt gel polymer electrolyte with 3D cross-linked polymer network for dendrite-free lithium metal batteries. *Adv Sci (Weinh)* 2018;5:1800559. DOI PubMed PMC
130. Wu J, Ling S, Yang Q, Li H, Xu X, Chen L. Forming solid electrolyte interphase in situ in an ionic conducting $\text{Li}_{1.5}\text{Al}_{0.5}\text{Ge}_{1.5}(\text{PO}_4)_3$ - polypropylene (PP) based separator for Li-ion batteries. *Chinese Phys B* 2016;25:078204. DOI
131. Liu J, Zhou J, Wang M, Niu C, Qian T, Yan C. A functional-gradient-structured ultrahigh modulus solid polymer electrolyte for all-solid-state lithium metal batteries. *J Mater Chem A* 2019;7:24477-85. DOI
132. Wang WP, Zhang J, Yin YX, et al. A rational reconfiguration of electrolyte for high-energy and long-life lithium-chalcogen batteries. *Adv Mater* 2020;32:e2000302. DOI PubMed